

The Wisconsin Method of
SCATT Wind Ambiguity Removal

Final Report for NASA Grant NAG 1-118
Development of an Algorithm for Removal of Directional Ambiguity
from Microwave Scatter Surface Wind Measurements for NOSS

Donald P. Wylie and Barry B. Hinton

Space Science and Engineering Center
University of Wisconsin-Madison
1225 West Dayton Street
Madison, Wisconsin 53706

October 1982

Abstract

We developed a method to remove spurious SCATT vectors from the multiple solutions (aliases) obtained for each resolution cell. In blind tests this method proved 96.3% to 98.8% accurate.

Using standard methods for analyzing meteorological data, it was found that large-scale (1° or larger) wind patterns could be extracted from the SCATT data using only the highest probability vectors in each NOSS cell with some filtering. Smaller scale features of the wind field are restored with repeated streamline analyses and editing of the NOSS vectors in which vectors most nearly conforming to the streamline analysis are retained and others are discarded. We conclude that the SCATT sensor could provide wind data of the highest resolution and quality known to meteorologists and oceanographers if these ambiguity removal methods were employed.

The Wisconsin Wind Ambiguity Removal Method

I. INTRODUCTION

Our approach was to edit the NOSS vectors according to smoothed streamline analyses of the high probability vectors. The philosophy is that the basic streamline patterns could be defined by using only the vectors with the highest probabilities in each cell (first alias). Other compatible aliases were introduced where the first alias conflicted with the streamlines; after which, re-analyses of the streamlines produced finer details of the wind patterns. In summary, this was an iterative procedure that contained two basic steps: an objective streamline analysis, followed by an editor that selected the NOSS vector closest in direction to the streamlines from each cell. These steps were repeated several times to converge on the wind field.

Obviously the first aliases or highest probability vectors were not the best choices in all groups. For this reason we employed objective analysis techniques designed for making field analyses from noisy data, or data containing some erroneous measurements. These techniques use averaging or smoothing functions to minimize the affects of bad observations.

In the course of development of our algorithm, a slight change in the philosophy of our method was made. In the first data set we selected only NOSS aliases that agreed with our streamline analyses, making no choices where none of the aliases were close to the streamlines (45° on first pass, followed by 20°). Our intent was to select only the NOSS cells where we had a high degree of confidence in the chosen alias. This decision was made because 75% of the first aliases were excellent measurements that

agreed with neighboring cells and produced far better wind coverage than any other data we have seen. The number of cells where no aliases were picked was small, 11%, when compared to the quantity of bad measurements from other data sources. We also felt that the scatterometer may not have produced any good alias for some cells, especially in low winds. Thus we discarded some of the data.

For the second data set, the blind set, we modified our algorithm to pick one alias from each cell, even if there was some directional disagreement. Cells where winds less than 2.0 m/s were found were discarded from the data set in the initial determination of the ambiguities in the scatterometer simulation at Langley. Thus we did not have to edit these cells in the ambiguity removal algorithm. This modification resulted in streamline analyses having more fine scale structure, and raised our skill in correctly selecting NOSS alias to 97.5% of the cells.

Most of the report discusses the first data set because we were given the true wind directions with the NOSS data and made extensive evaluations of our method. The second or blind data set was evaluated by the Langley Research Center, and their findings are given in summary form.

II. DESCRIPTION OF THE METHOD

The first step of the method was to rank all vectors in each cell according to their probabilities to find the first alias. Where all vectors had equal probabilities, the cells were ignored for the first analysis and no first alias was assigned.

The Barnes low pass filter technique (Barnes 1973) was used to make objective analyses of the U and V components of the first aliases at uniformly spaced grid points. The Barnes method filled each grid point with the average of all wind vectors weighted according to their distance

from the grid point. An inverse exponential weighting function was used (Fig. 1).

The degree of detail represented in the analyzed wind field could be regulated by varying the grid point spacing and the width of the weighting function. By using a high resolution grid and a narrow weighting function, the analyzed field could describe all of the measurements in detail. However, this was not desired because the analyzed field would then contain all of the noise in the original data. By experimenting with different grid resolutions, we found that a grid spacing of 1° latitude and longitude, with the weighting function shown in Figure 1, produced streamline patterns that depicted well most desired features of the wind field (See Fig. 2). For our examination of the results, the objectively analyzed streamlines were plotted from the U and V component grids using the method described by Whittaker (1977). This monitoring was part of the algorithm development processes, and was not used on the blind data set.

The second step was to remove all NOSS vectors that deviated substantially from the wind direction of the objectively analyzed field. The editing was done objectively by the computer. For the first pass we eliminated all vectors deviating more than $\pm 45^\circ$ from the analyzed wind direction. These discarded first aliases were then effectively replaced with lower probability aliases that conformed to the streamline analysis. The order of 25% of the first aliases were tentatively discarded in this step.

The second iteration repeated the objective analysis on all of the vectors that passed the first iteration. The same grid spacing and weighting function was used. This new analysis was used to re-edit the NOSS field with a criteria of $\pm 20^\circ$ in direction. Note that if no alias

conformed more closely than $\pm 20^\circ$, no alias was selected. Such a cell was coded with a "no pick" flag.

This method was initially carried through five iterations on the starter data set (Rev 825), but little change in the analysis field appeared after the second iteration. Experiments were tried with different editing criteria and $45^\circ/20^\circ$ criteria was chosen as an optimum match for the first data set. In the second blind data set, we dropped the $45^\circ/20^\circ$ criteria and chose the vector closest to the streamline from each cell which eliminated the no pick class

The editing criteria had only a small influence on the resulting fields. The purpose of using a 45° criteria on the first pass was to eliminate most of the obviously wrong choices from the field, and leave the fine tuning to a second pass. It was our experience that most of the streamline patterns were determined from the objective analysis of the first aliases. The second pass changed minor details inside the initial patterns only in the blind data set where cells with aliases that deviated substantially from the streamlines had to be included because they were closest. These cells forced fine-scale details in the streamlines that were not obtained from the first analysis of the first alias.

III. RESULTS

The results are presented as two groups: the initial data set where NOSS cells of the no pick class were dropped from the wind analysis, and the blind data set where all cells were included.

A. Initial Data Set

To judge the accuracy of our method, each surviving SCATT vector was compared to the direction of the truth field vector given with the data set. All vectors that were within $\pm 20^\circ$ of the truth vector were

categorized as good picks and vectors outside of this range were labelled as bad picks (Table 1). In addition, as mentioned above, we had several vector groups from which no vector choices were made (no picks). The error in our method was the bad pick statistic. The no pick cells were considered to be without any alias that represented the wind field. Thus, our total error would have to include all of the no pick cells. Within the good and bad pick categories, we listed in Table 1 the number of first alias vectors present. It is apparent that the majority of good picks were first aliases to start with, ranging from 70.4 % to 76.7% of the total number of cells. The first alias vectors that were bad picks were only 1.6% to 2.3% of the total. This affirms our supposition that the high probability vectors could be used as a starting point.

The bad picks were either light winds or areas where sharp directional changes occurred. The subtropical highs and cols (deformation zones) were also more difficult to analyze with these data. However, these features have been difficult to analyze with all other meteorological data because of their variable wind directions and generally unorganized nature.

The objective analysis scheme used here tended to broaden features by smoothing the input observations. Thus, where small scale directional changes were present with light winds, more bad picks or no picks occurred.

Similarly, in a few areas of strong winds, no picks occurred where there was a strong shear zone or area of sharp directional turning.

A detailed description of each case follows:

.The Starter Set, Rev 825. Because of the length of the orbit, we were forced to break 825 into two sections and made separate analyses of each. The major problem encountered was on the lower part of the orbit

where the westerly winds (blowing from west toward the east) changed to northeasterly winds (Fig. 2). This is a subtropical high area, and the locations of the no picks are indicated by arrows in the margins.

The upper part of the orbit contained westerly winds and a double low or pair of cyclonic vortices (Fig. 3). These features were diagnosed in our streamline analysis; however, most of the no picks and bad picks were around the double vortices. A few also occurred on the left side of the left track around the vortex at the top of the track.

From the streamline analyses we concluded that the major features of this orbit were resolved to 1° and the errors were minor points of these features.

.Case 1, Rev 1093. There were only two principal features of 1093: a low or cyclonic vortex on the upper left side, and a shear zone on the lower left side which may have been a cold front (Fig. 4). Our major problem was in the shear zone. Most of the bad picks and no picks were in this area because of the inability of the streamline analysis to resolve a tight gradient in the wind field. Other no picks occurred east of the vortex on the right side, also, where the directional changes were large.

The general features of this area were properly diagnosed by the analysis. Our analysis adequately handled this data set, as it did the previous set.

.Case 2, Rev 1298. This case was broken into two parts, as was done for Rev 825. The upper section contained a large anticyclonic vortex with an edge of another cyclonic vortex on the fringe of the right track (Fig. 5). Our analysis correctly diagnosed this feature. A very small number of bad picks were made, mainly on the right track (Fig. 5).

The lower part contained a col (deformation) on the left track and part of a cyclonic vortex on the right track. Most of the bad and no picks occurred in and southwest of the col area, as indicated by the arrow (Fig. 5).

.Case 3, Rev 1140. This case contained a cyclonic vortex on the upper part of the right track and large complicated anticyclonic vortex (probably a subtropical high) on the southern part of the orbit (Fig. 6). Our method found the cyclonic vortex on the upper part of the orbit, but failed to diagnose it as a closed circulation. This resulted from too few first choice winds on the right side of the vortex. The analysis produced a vortex which opened toward the east. Had other data been available to the east, this error might have been avoided.

The majority of bad picks and no picks were made in the anticyclonic vortex to the south. Most of the major features of the pattern were correctly diagnosed, but the finer points were poorly handled. The reason was probably the quality of the first alias vectors.

In an attempt to improve the quality of our first guess field, we changed the criteria for selection of the first alias vectors. The criteria was upgraded from selecting just the highest probability vector in each group to further require this vector to have a probability 1% greater than other vectors in the group. This eliminated many of the groups with nearly equal probabilities. The resulting fields also are shown in

Figure 6. It is apparent that this exercise did not improve the first guess field and made the streamline analysis worse.

We concluded that our analysis could not be improved in this way, and the 1% criterion was dropped. In areas where probabilities were nearly equal, our analysis would be poorer, but little can be done about this.

.Case 4, Rev 1183. The major feature of this case was a large anticyclonic vortex fully covered by the orbit. Our analysis correctly found this feature; however, the complicated pattern to the southwest was difficult to resolve. Many of the no picks and bad picks occurred in this area (Fig. 7).

Our analysis appeared to resolve the major features of this case with the errors mainly appearing in areas of sharp changes, as discussed earlier.

.Case 5, Rev 1298. A vortex in the upper part of the orbit and a shear line on the lower section, where westerly winds changed to northerly winds, gave us problems (Fig. 8). As in the previous two cases, most of the bad and no picks occurred where the first choice winds were scattered in direction. However, the majority of this orbit was correctly diagnosed because of the large areas with strong winds of uniform direction that defined the large scale pattern.

.Case 6, Rev 1140. A similar large anticyclonic vortex dominated this orbit with smaller features to the north (Fig. 9). Our analysis resolved the major features of this orbit as expected.

Most of the bad and no picks occurred on the outer edges of the swaths. It was obvious that the greatest difficulty occurred on these edges. The streamline program appeared good at finding areas where the first choice winds were in agreement, and smoothly interpolating between

these areas. However, on the edges of the swath the program had to extrapolate gradients because of the lack of bounding information. This increased the probability of making errors.

B. The Blind Data Set

The blind set consisted of five cases with the truth winds withheld. Thus, we ran our algorithm on all five cases without knowing the quality of its performance or being able to fine tune its operation for special features in the data.

The algorithm was modified to pick one alias from each cell, regardless of the difference between the streamline direction and the best alias as previously mentioned. In the second iteration, the streamline analysis was made, using one alias from each cell. We found that the best winds in questionable cells that would previously have been rejected as no picks improved the wind field in most areas. This illustrated the ability of the scatterometer to resolve the fine scale structure in the wind field.

Most of the bad picks made by the revised algorithm were made along lines of confluence or diffluence, or where tight vortices were present. The errors tended to occur in groups of 5-12 cells. The chosen aliases in these cells were usually in the same quadrant ($\pm 45^\circ$) as the truth wind or the best alias. This indicates that the algorithm recovered the large scale (> 100 km) features of the wind field, with the errors being minor deviations from the broad patterns which were not resolved by the algorithm.

Detailed discussions of each case follow:

.Case 1. Westerly winds off the east coast of North America were recovered from the algorithm for a majority of the cells. Two problem areas occurred southeast of New Foundland where confluence lines between

northerly and southerly winds occurred. The algorithm picked northwesterly aliases where more northerly aliases were appropriate. A similar problem was found with four vectors to the north on the right side swath. Other errors occurred on the southern end of the right swath where the winds were light. These appear to be in an area where large directional changes occurred due to the light winds.

.Case 2. A large cyclonic vortex southeast of Greenland was centered between the two swaths of the satellite. Very few errors were made, which is surprising because large wind direction changes appeared on the right swath south of the low. The errors occurred in small groups of two to five vectors along the lines of maximum shear. Another shear line caused six errors on the left swath where the winds were light. The algorithm had its best performance on this case.

.Case 3. Four large shear areas also appeared in Case 3, which cause errors in our ambiguity choices. The streamline analyses picked up the wind patterns, but missed the locations of the shear lines by one or two NOSS grid cells. The aliases that were picked were close to the best alias, indicating that the streamline pattern was close to the truth field. The errors occurred because of the smoothing function (low pass filter) built into the streamline analysis method.

.Case 4. A large cyclone with strong winds appeared on the lower right side swath. Our algorithm missed four vectors in the center of the cyclone because the streamline analysis located the cyclone two NOSS cells to the north. Two other groups of numerous bad picks occurred on the outer edge of the left swath. In these areas the streamline analysis found a smooth southwesterly flow where a more westerly choice should have been made. The directional error made by the algorithm was small ($< 45^\circ$). More

data to the west would have helped our analysis. With some confusion in the first aliases on the swath edge, the streamline analysis extrapolated gradients in the winds toward the edge. Thus, a smooth analysis was made where some wind pattern detail occurred.

.Case 5. Another example of a strong cyclonic vortex appeared in the right swath. Our streamline analysis mislocated this vortex by two cells to the north, causing four bad picks. To the west of the vortex, a large group of bad picks occurred in a light wind area. It appears that aliases close to the best choice were selected as in the previous case, and bad picks resulted from some confusion in the first aliases in that area.

IV. VORTICITY AND DIVERGENCE FIELDS

Vorticity and divergence analyses were made on Cases 5 and 6 of the initial data set (Fig. 15). The analyses made on our ambiguity removed SCATT fields tended to closely resemble the truth fields. This was encouraging and indicated that our method produced wind fields that were basically correct in their major features.

As a second measure of the quality of the analyses, we made scatter plots of the divergence values for each 1° grid point as a function of the vorticity values (Fig. 15). From the patterns shown, it appeared that vorticity and divergences were mostly unrelated. This notion is given to the viewer because the maxima and minima of each pattern are found in different locations. But from Ekman boundary layer theory, we would expect some convergence to occur with cyclonic vorticity. The scatter plots show that this is the case and the vorticity and divergence have some relationship. The correlation of the two on a grid point basis was approximately 0.5 to 0.6.

V. SPATIAL CORRELATIONS

As another measure of the quality of the simulated SCATT wind fields, the auto correlation functions were calculated for three cases, both the truth and analyzed fields (Fig. 16). A fairly broad correlation was found for both types of data. The high correlations for close distances (< 100 km) indicate that there were little changes between neighboring vectors. Thus, the 50 km sampling represented an "overkill" of information.

The width of the correlation is roughly comparable to the auto correlation of ship wind measurements (Fig. 17). The ship and cloud correlation functions were made over the tropical Indian Ocean during the summer of 1979 (Wylie and Hinton 1981). By comparing Figures 16 and 17, one can see that the cloud motion data have a broader correlation. This is not a surprise because cloud motions represent winds above the boundary layer, and thus we did not expect to see many shear lines or other small scale features.

VI. CONCLUSION AND RECOMMENDATIONS

We conclude, on the basis of the information in Table 1, that the method used on the blind data set worked quite well. The success of this relatively simple method derives in large measure from the skill of the simulated SCATT.

We recommend that a similar method be further developed if a scatterometer mission is undertaken. It would be desirable to study the tradeoff between the percent of good picks and scatterometer skill. This study would benefit plans for a data processing system which could allow for poorer than planned instrument performance, or degradation over time.

In detailed studies of atmospheric phenomena, where data processing speed is less of a constraint, the method would benefit from any high quality data that could be used near the outer edges of the swath. However, data of lower quality (e.g., ships of opportunity) might have a negative impact on ambiguity removal when there are small angles between available aliases. When to use auxilliary data could be determined from simulated SCATT data and simulated surface observations randomized with appropriate error characteristics.

References

- Barnes, S.L., 1973: Mesoscale objective map analysis using weighted time-series observations. NOAA Tech. Memo. ERL NSSL-62, 60 pp.
- Whittaker, T.M., 1977: Automated streamline analysis. Mon. Wea. Rev. 6, 786-788.
- Wylie, D.P., and B.B. Hinton, 1981: The feasibility of estimating large-scale surface wind fields for the summer MONEX using cloud motion and ship data. Bound. Layer Met. 21, 357-367.

Table 1.
The Summary of the Total Numbers of Good and Bad Picks
Made from the Simulated SCATT Data Sets

<u>Case</u>	<u>Rev</u>	<u># Good Picks</u>		<u># Bad Picks</u>		<u>#No Picks</u>
		<u>1st Choices</u>	<u>All</u>	<u>1st Choices</u>	<u>All</u>	
<u>Initial Data Set</u>						
0	825	76.7%	83.5%	2.3%	5.9%	10.6%
1	1093	74.6%	83.2%	0.7%	6.2%	10.5%
2	1298	76.7%	87.6%	1.8%	6.0%	6.4%
3	1140	70.4%	79.4%	1.8%	9.6%	11.0%
4	1183	72.8%	81.5%	2.2%	7.1%	11.4%
5	1298	78.9%	88.9%	1.6%	4.3%	6.8%
6	1140	72.5%	82.9%	1.6%	5.3%	11.8%
<u>Blind Data Set</u>						
1		85.6%	96.3%	2.1%	3.7%	*
2		91.6%	98.8%	0.9%	1.2%	
3		88.8%	97.9%	0.8%	2.1%	
4		89.2%	96.8%	1.4%	3.2%	
5		90.4%	98.4%	0.8%	1.6%	

* Some NOSS cells were excluded from the Blind Set in the wind retrieval process before the application of this algorithm. Thus, the ambiguity removal algorithm was modified to accept all of the remaining cells in the Blind Set.

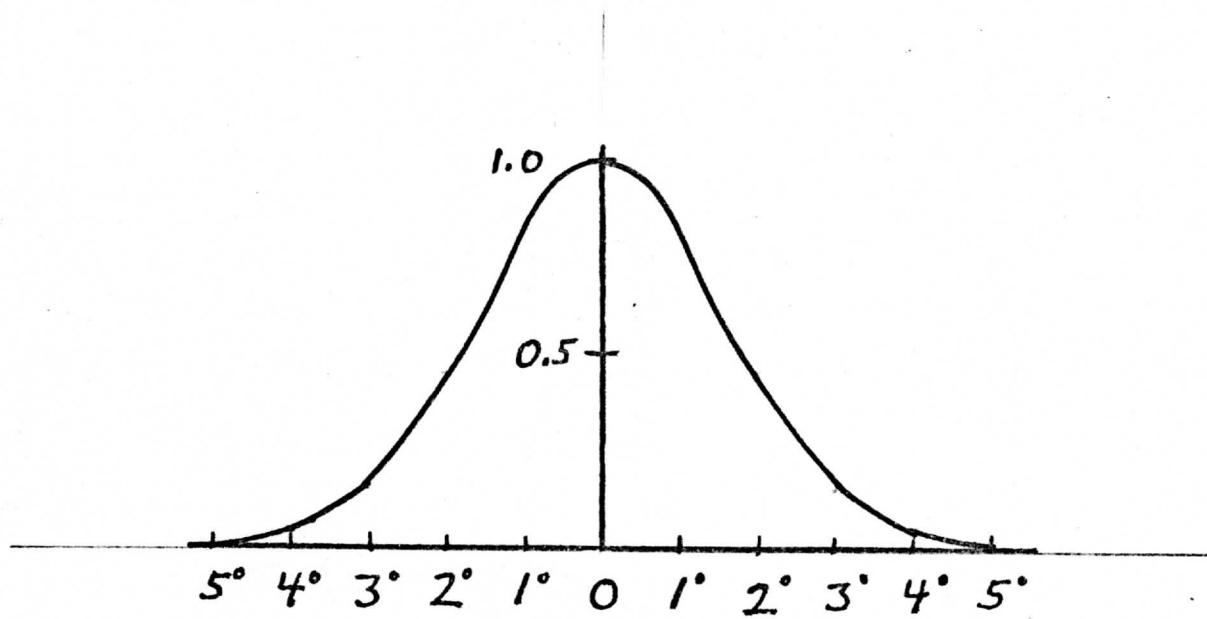


Figure 1: The weighting function used in the objective analysis program.

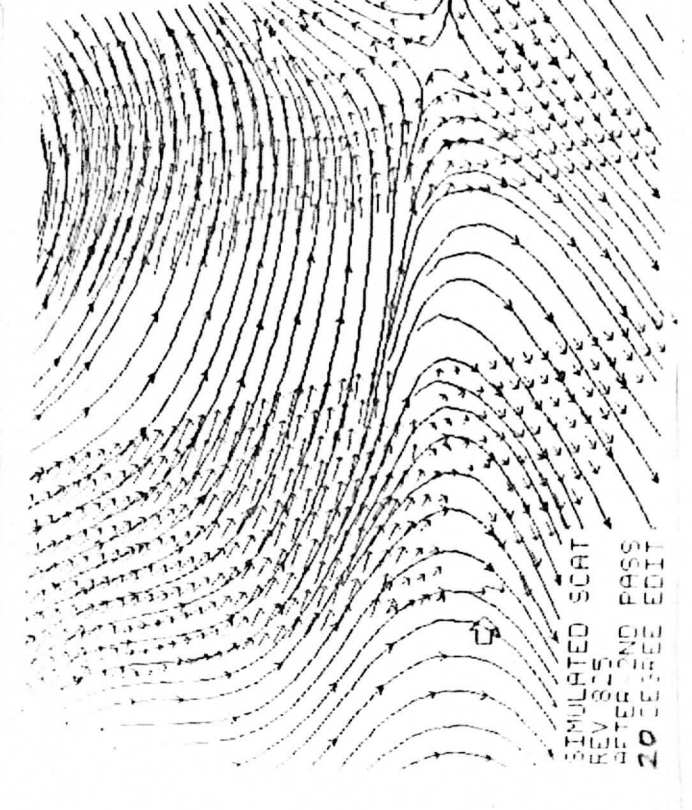
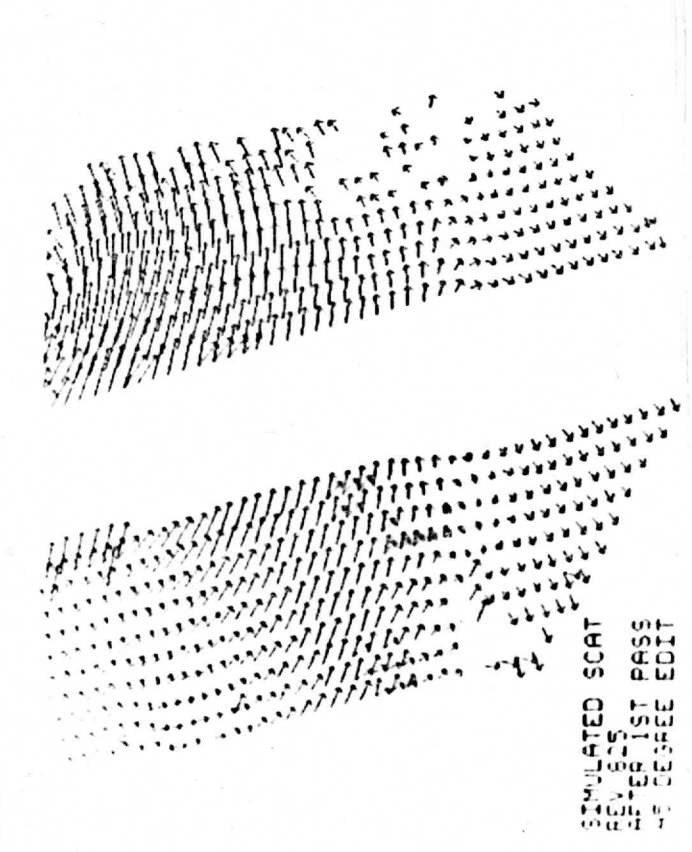
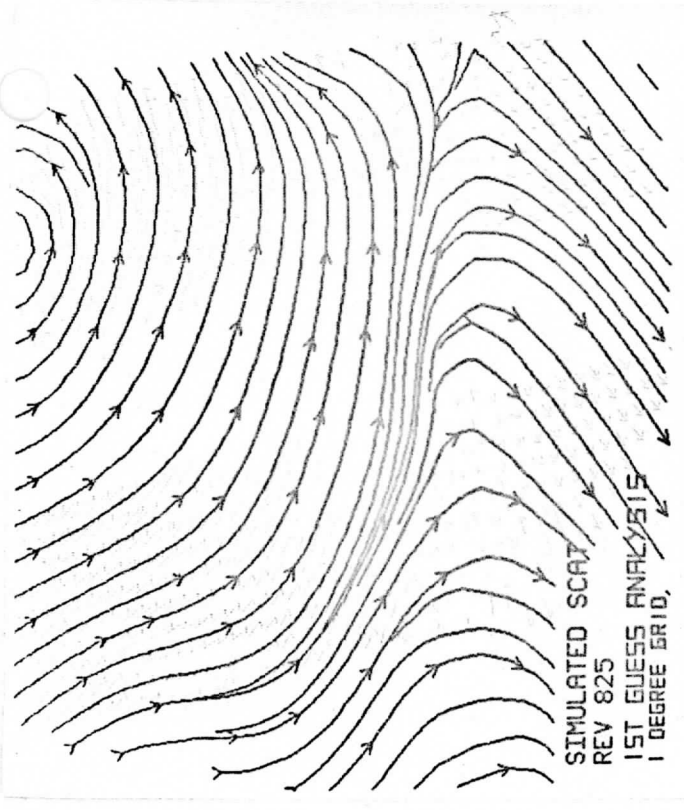
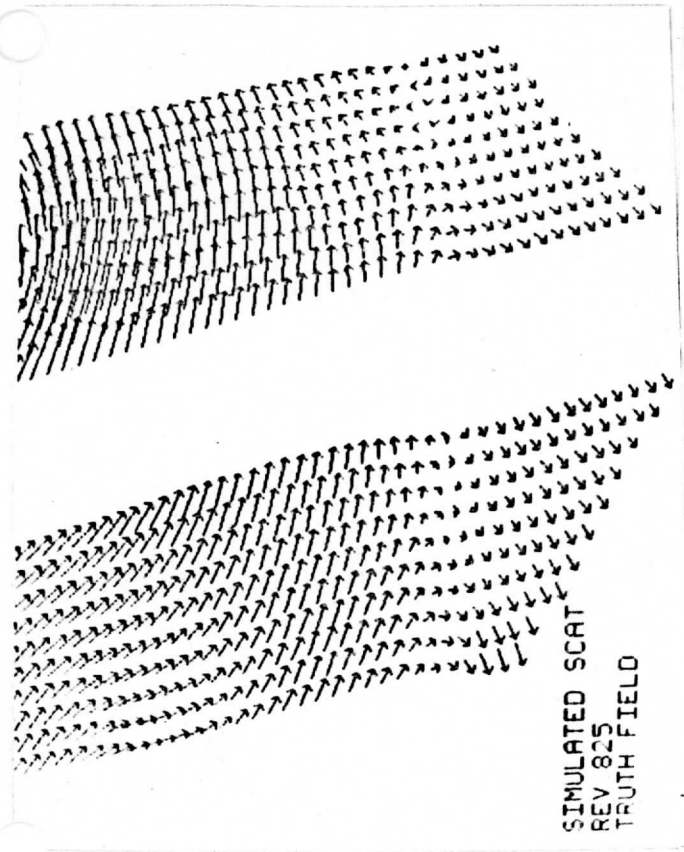
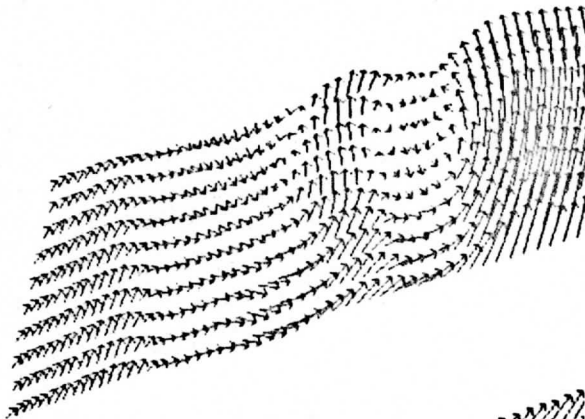
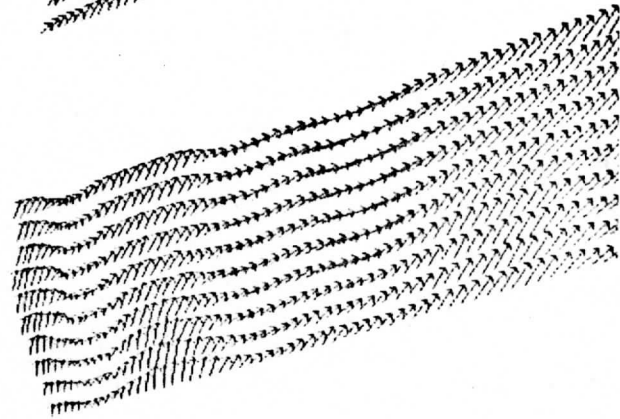


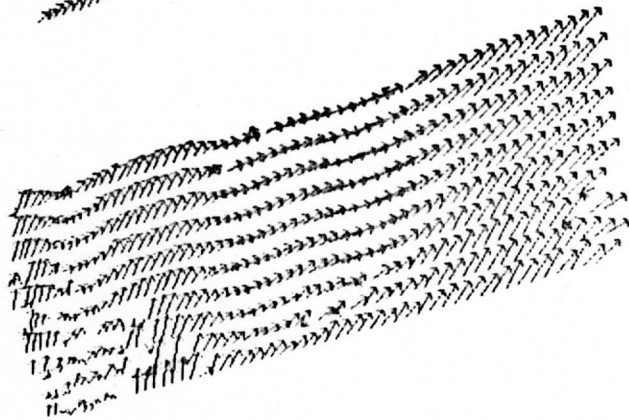
Figure 2: The starter data set Rev 825, lower half.

SIMULATED SCAT REV 825

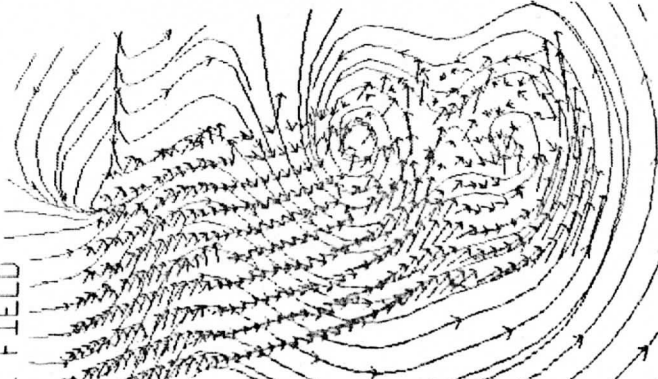
TRUTH FIELD



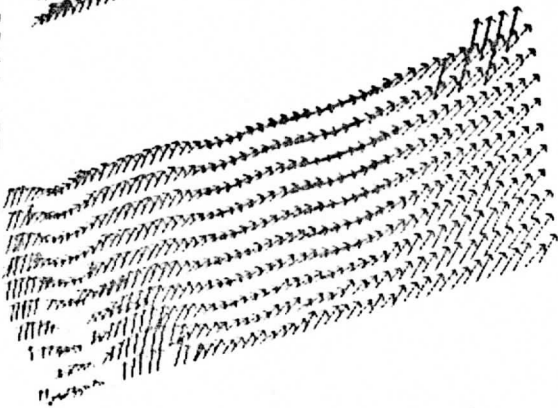
SIMULATED SCAT REV 825
FIRST CHOICE FIELD



SIMULATED SCAT REV 825
FIRST CHOICE FIELD



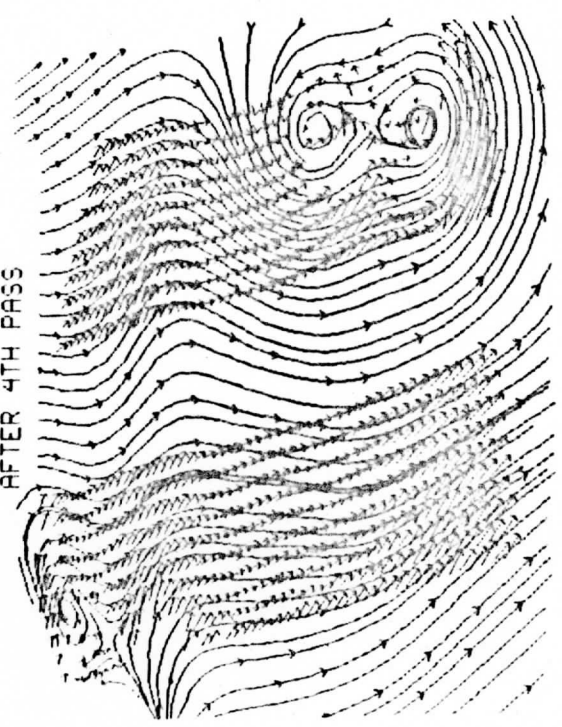
SIMULATED SCAT REV 825
AFTER 1ST PASS



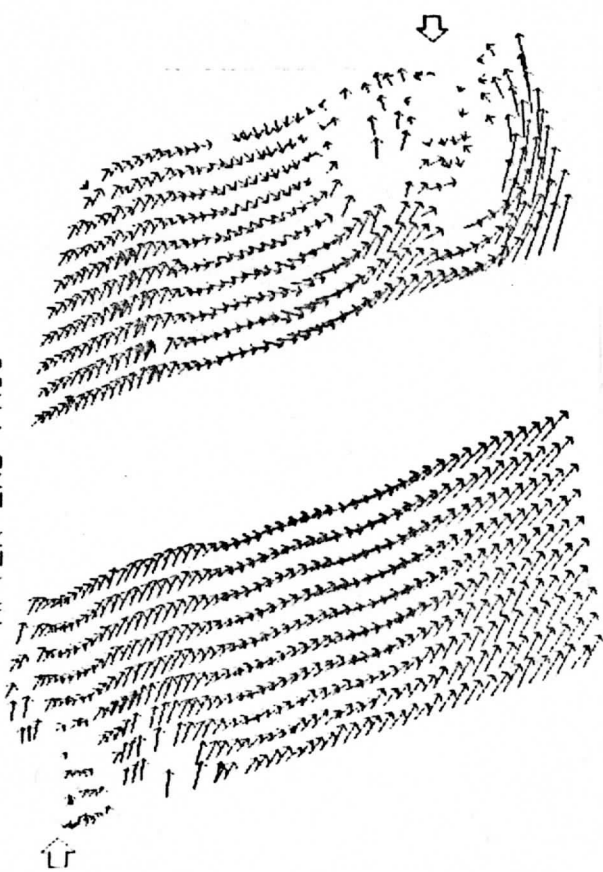
45 DEGREE EDIT

Figure 3: Rev 825 upper half.

SIMULATED SCAT REV 825
AFTER 4TH PASS



SIMULATED SCAT REV 825
AFTER 2ND PASS



SIMULATED SCAT REV 825
AFTER 5TH PASS

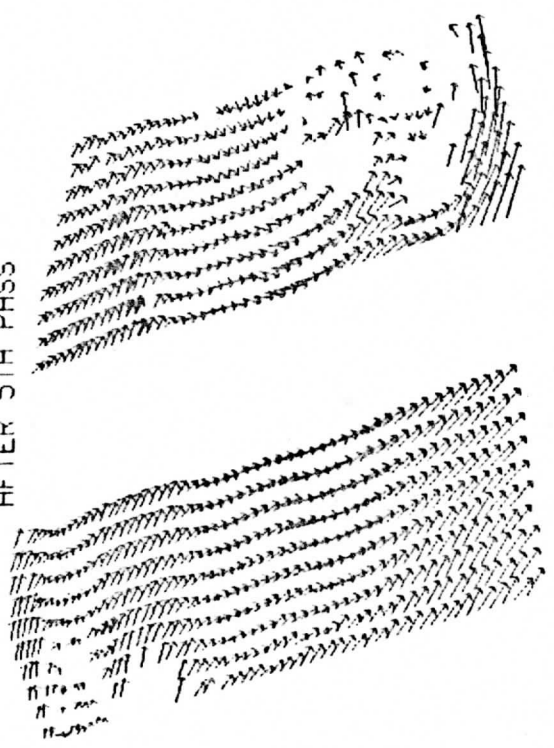


Figure 3 continued: Rev 825, upper half.

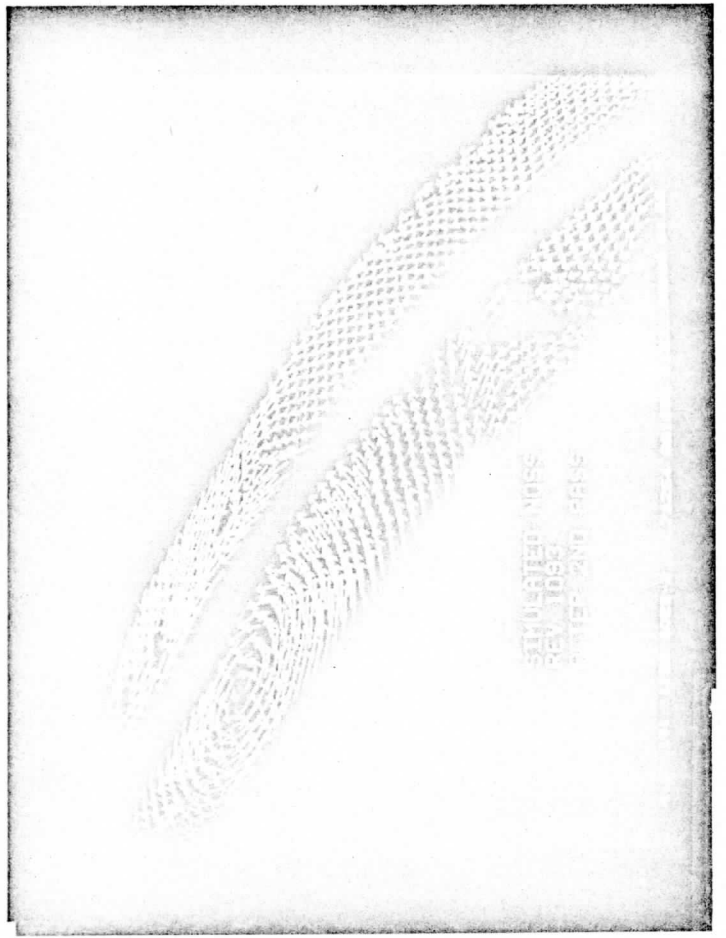
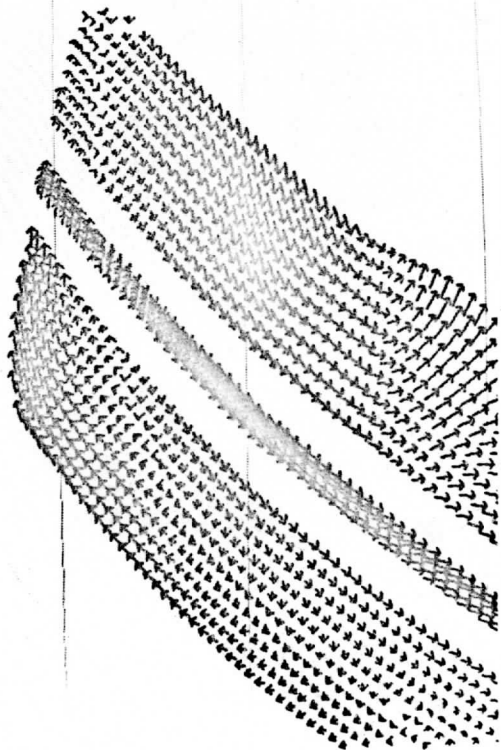
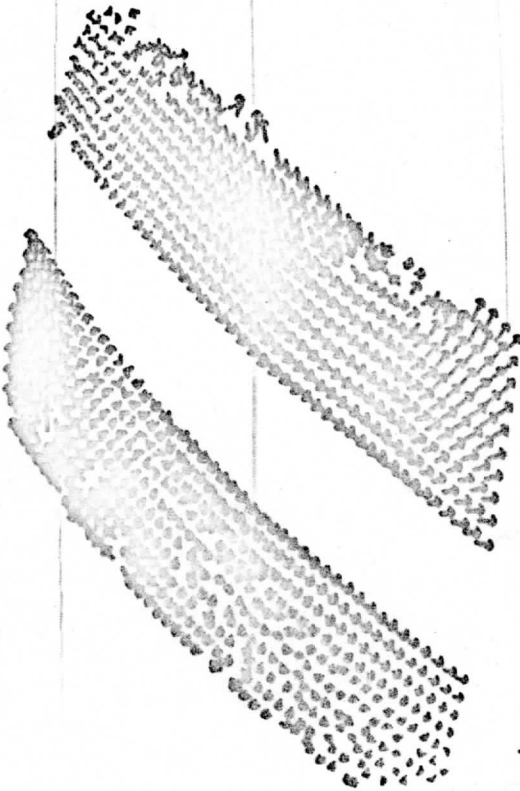


Figure 4: Case 1, Rev 1093.

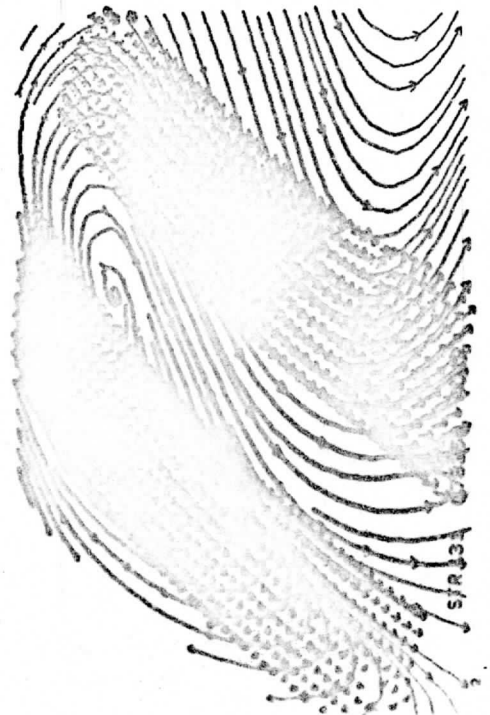
SIMULATED SCAT
REV 1298
TRUTH FIELD



SIMULATED SCAT
REV 1298
FIRST GUESS FIELD



SIMULATED SCAT
REV 1298
AFTER 1ST PASS



SIMULATED SCAT
REV 1298
AFTER 2ND PASS

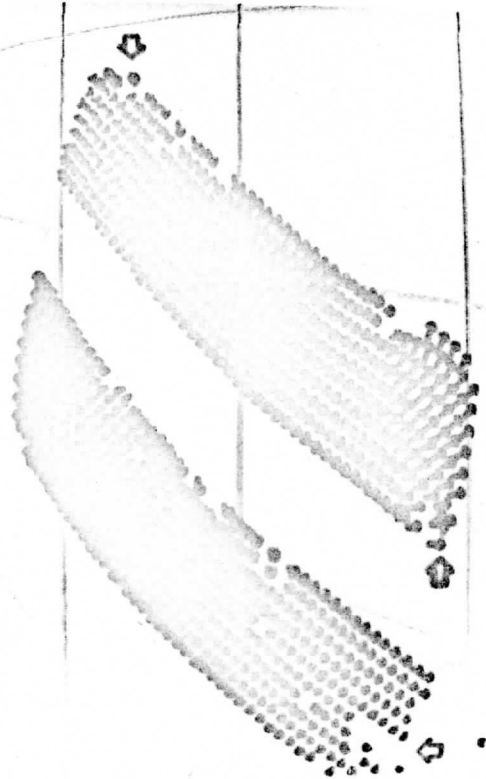
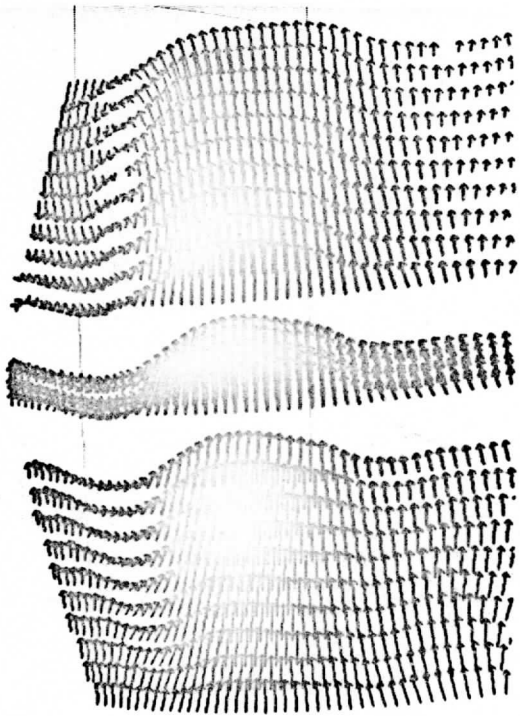


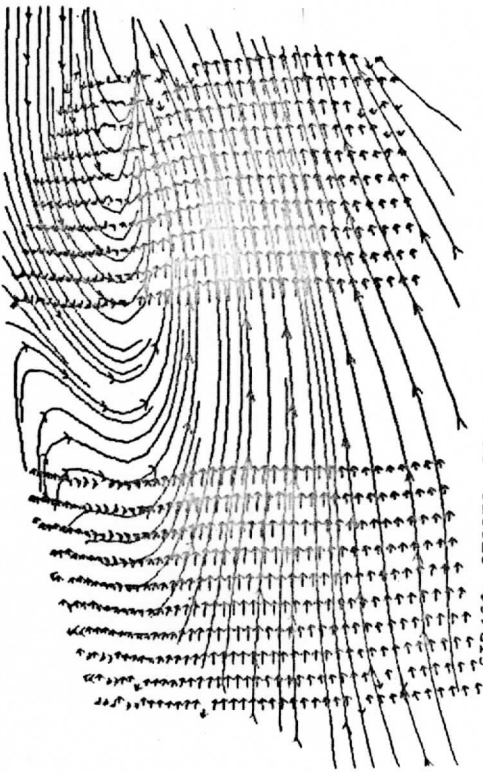
Figure 5: Case 2, Rev 1298, upper half.

SIMULATED SCATT
REV 1140
TRUTH FIELD



2

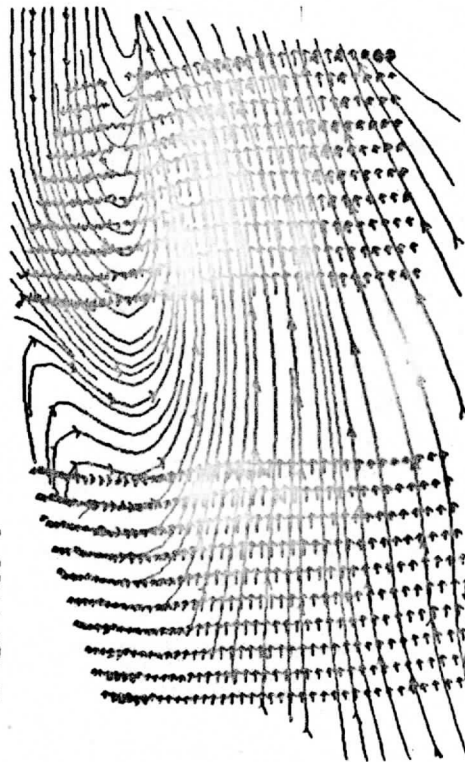
SIMULATED SCATT
REV 1140
FIRST GUESS



STR 100 078350 0011

1

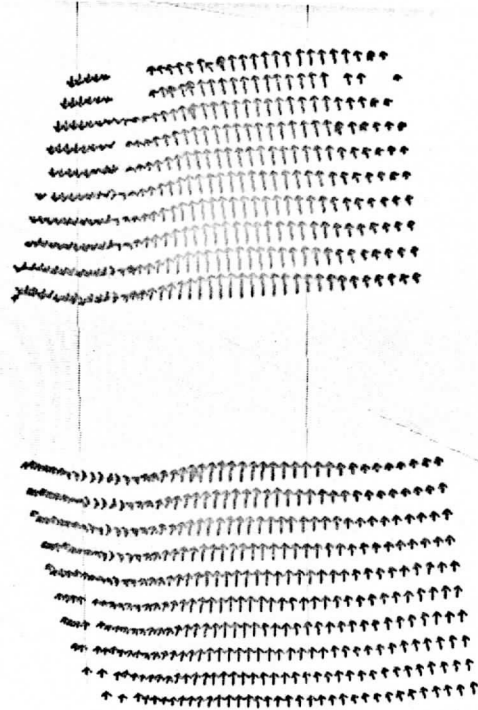
SIMULATED SCATT
REV 1140
AFTER PASS 1



STR 100 078350 0011

3

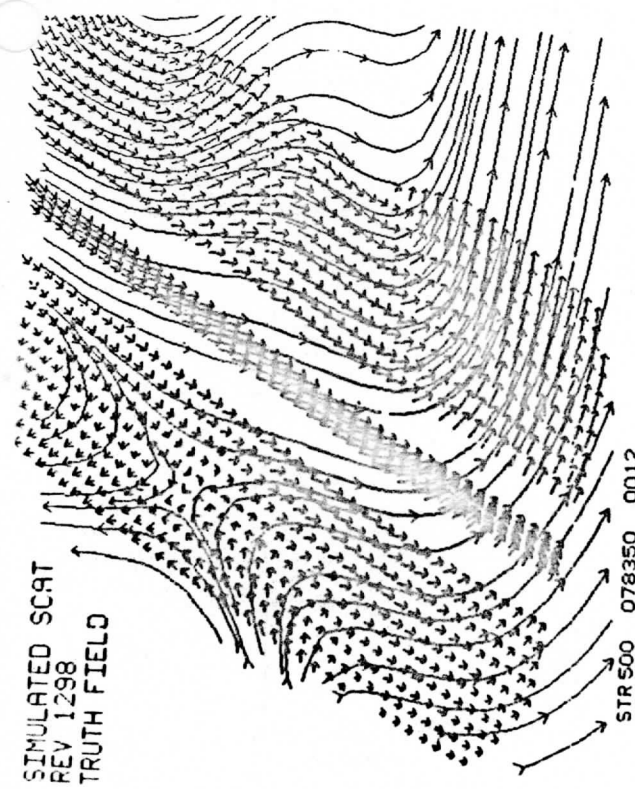
SIMULATED SCATT
REV 1140
AFTER PASS 2



4

Figure 6: Case 3, Rev 1140 upper half.

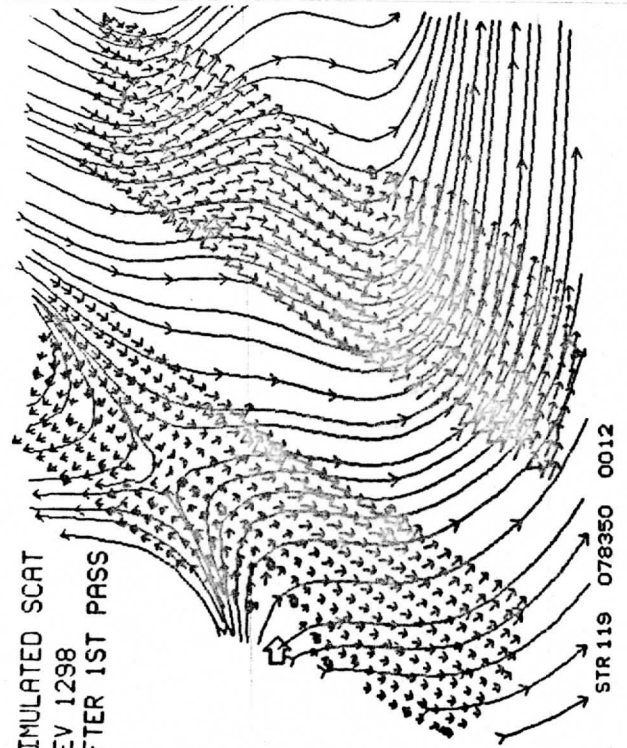
SIMULATED SCAT
REV 1298
TRUTH FIELD



STR 500 078350 0012

4

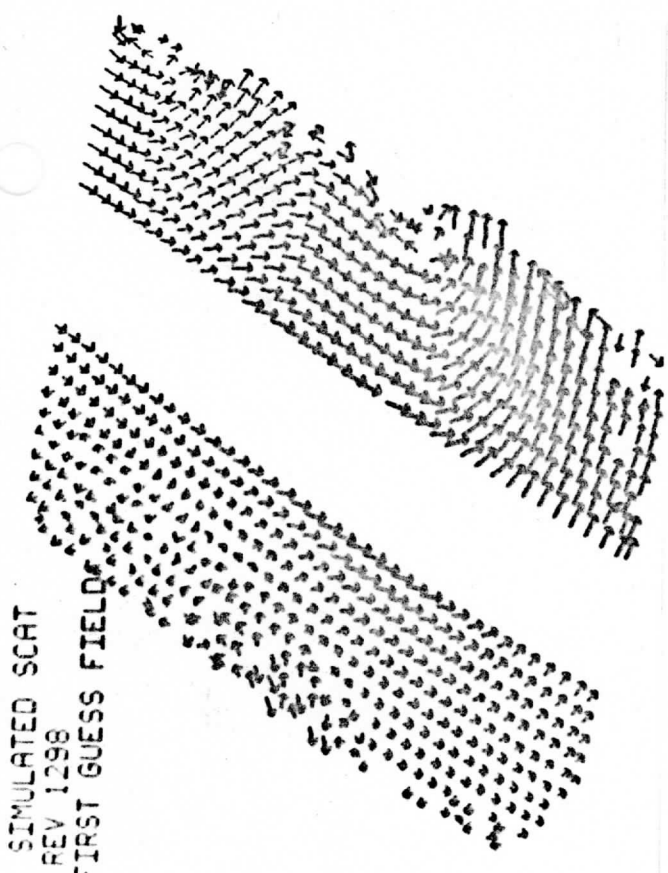
SIMULATED SCAT
REV 1298
AFTER 1ST PASS



STR 119 078350 0012

2

SIMULATED SCAT
REV 1298
FIRST GUESS FIELD



SIMULATED SCAT
REV 1298
AFTER 2ND PASS

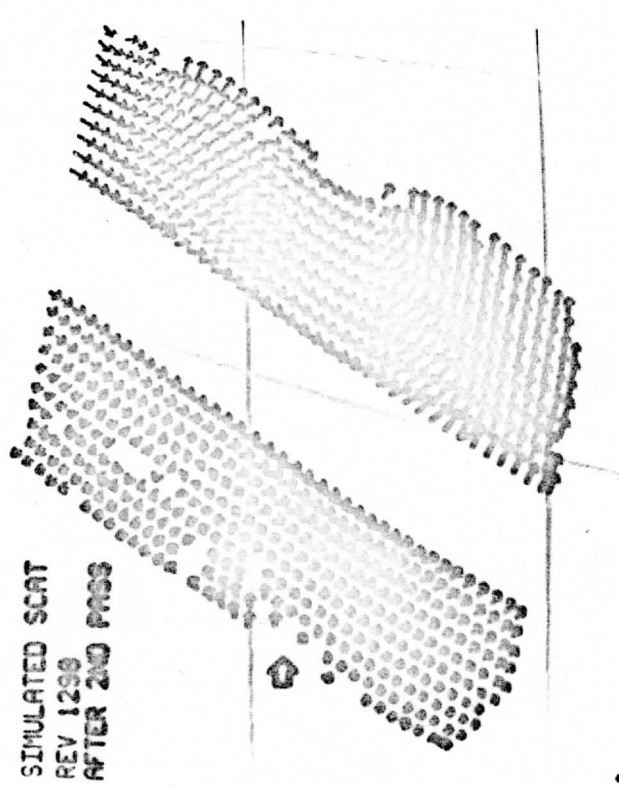
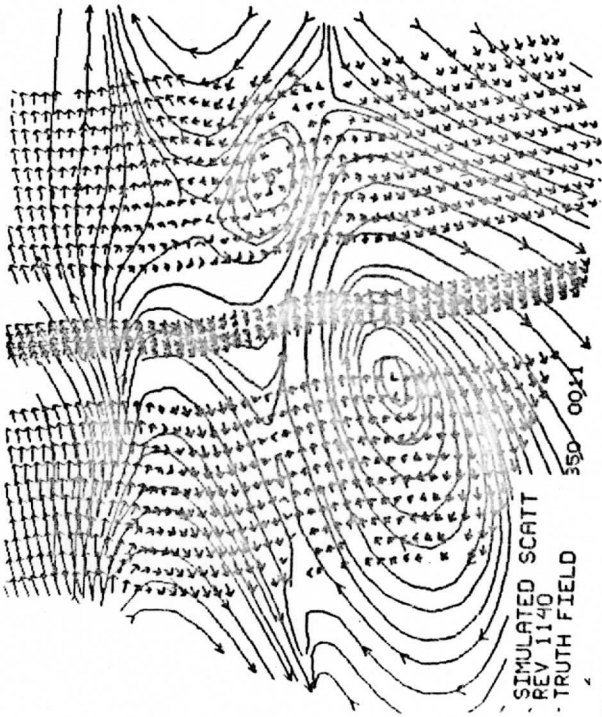
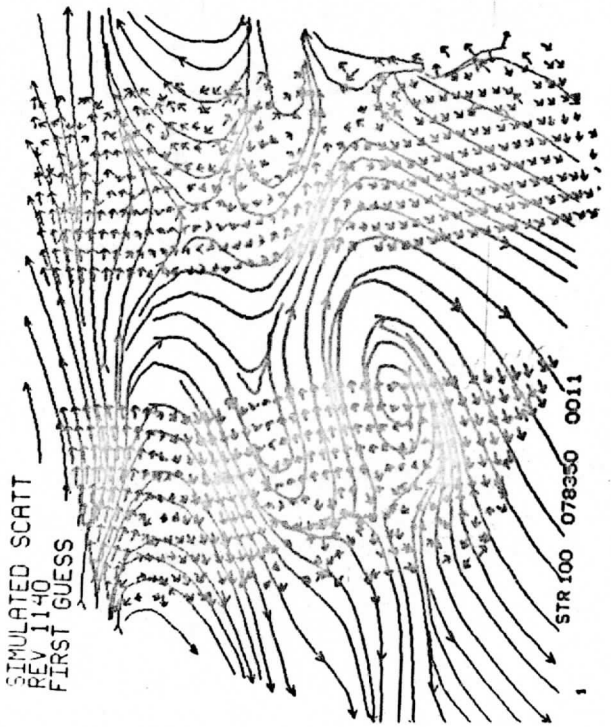


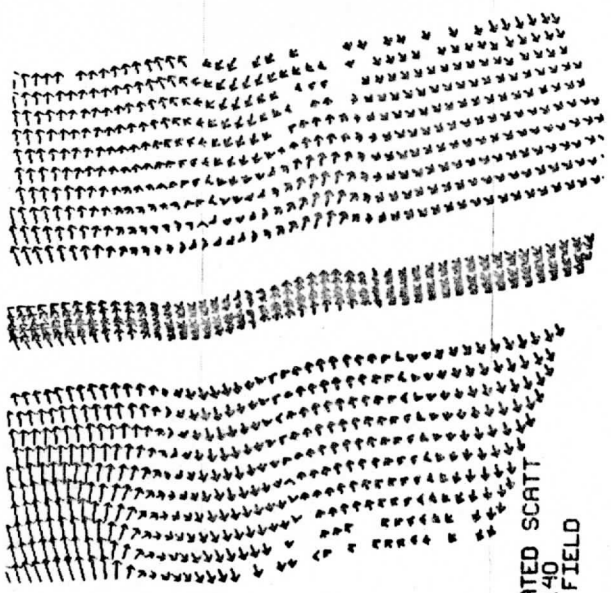
Figure 5 continued: Case 2, Rev 1298, lower half.



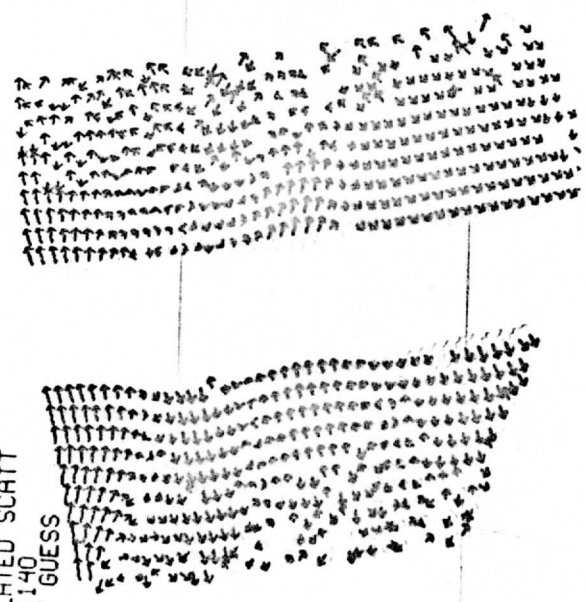
SIMULATED SCATT
REV 1140
TRUTH FIELD 350 0011



SIMULATED SCATT
REV 1140
FIRST GUESS STR 100 078350 0011



SIMULATED SCATT
REV 1140
TRUTH FIELD 2



SIMULATED SCATT
REV 1140
FIRST GUESS

Figure 6 continued: Case 3, Rev 1140 lower half.

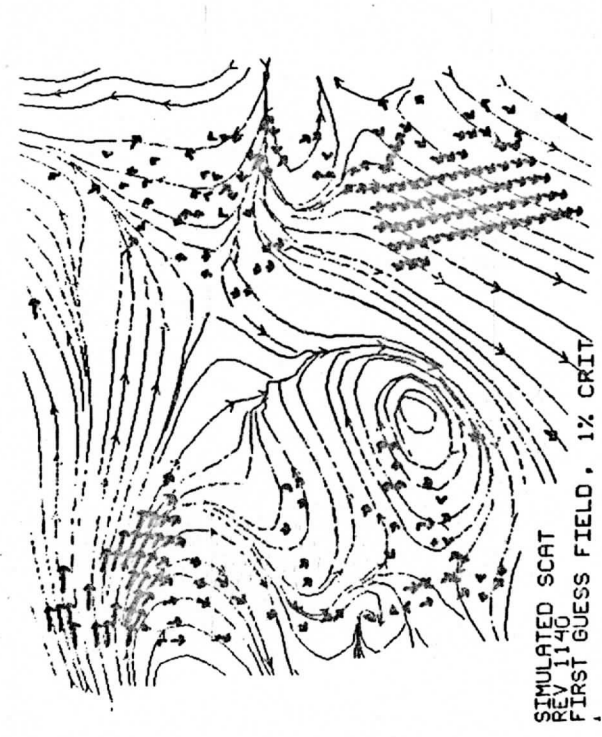
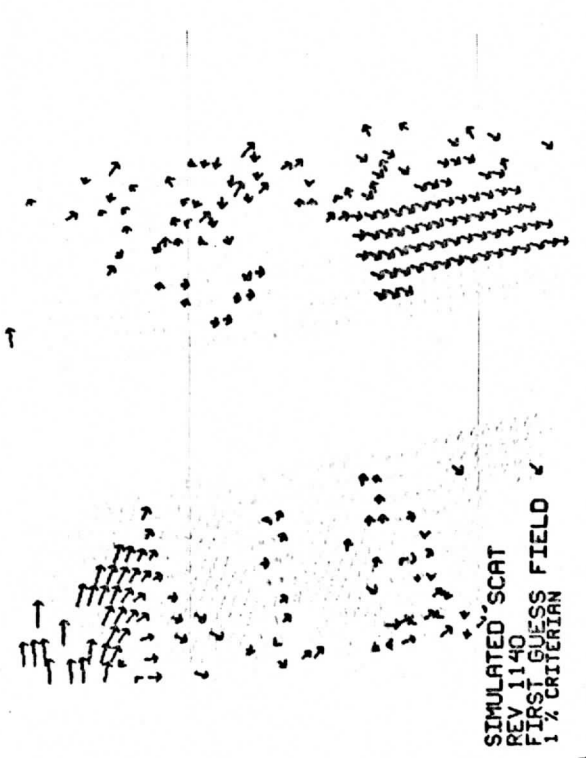
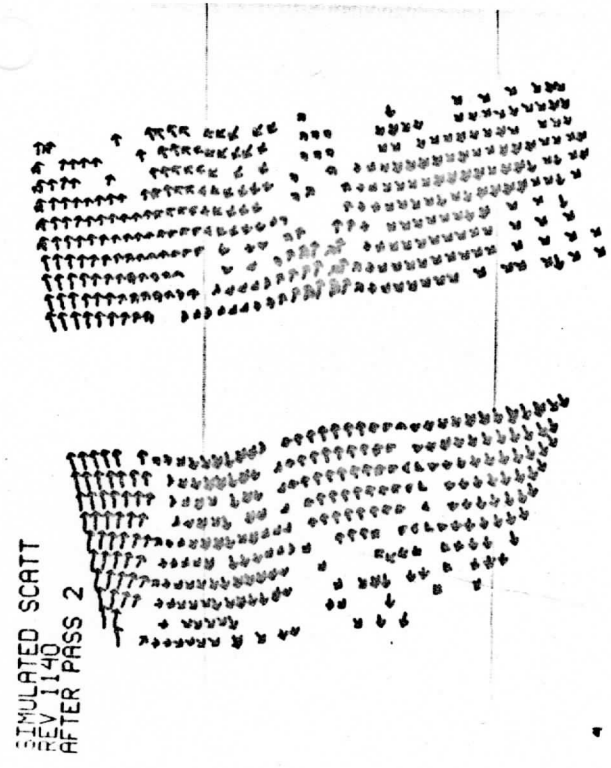
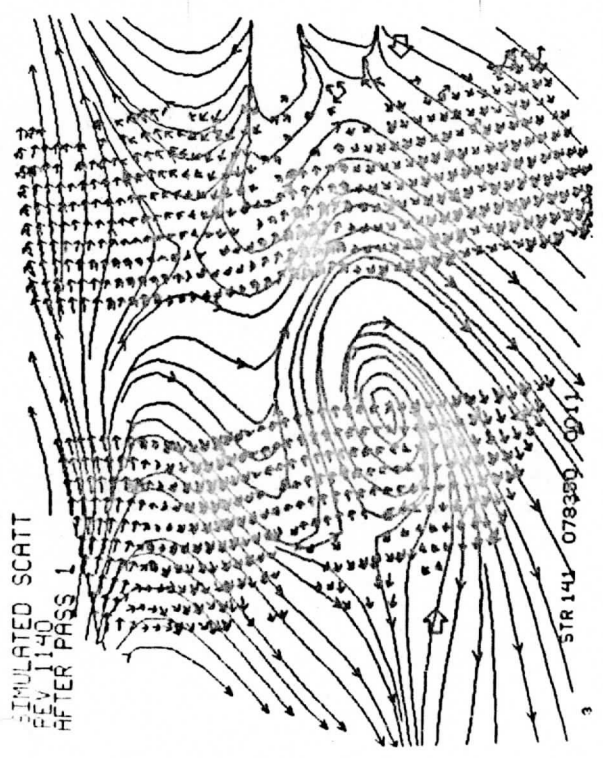
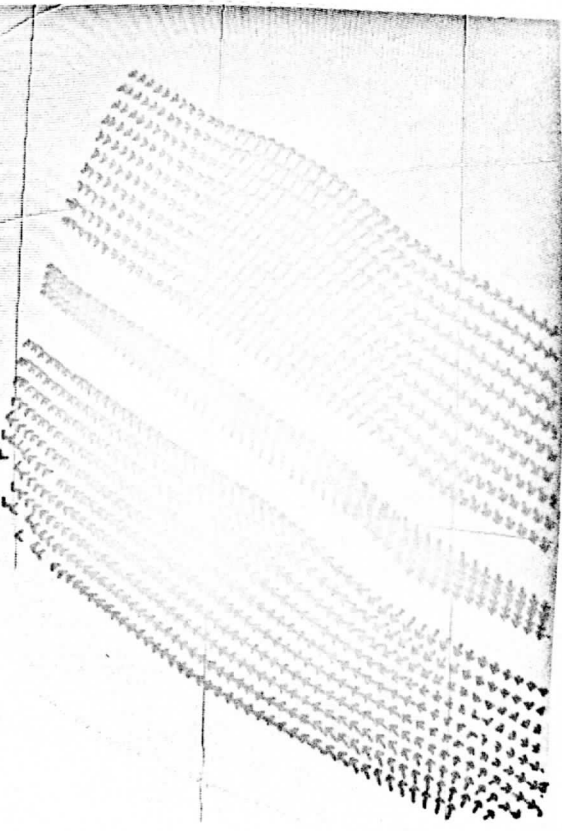
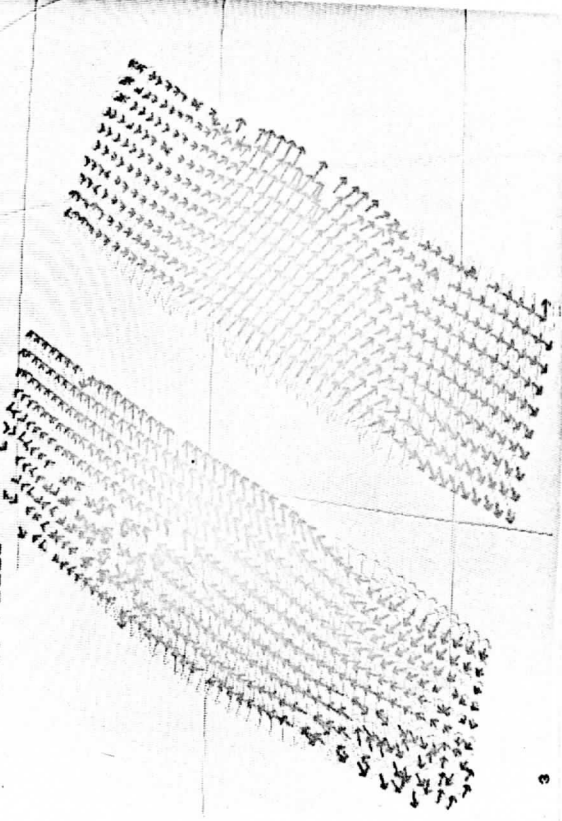


Figure 6 continued: Case 3, Rev 1140 lower half where the First Choice winds had probabilities >1% of the other vectors in their groups.

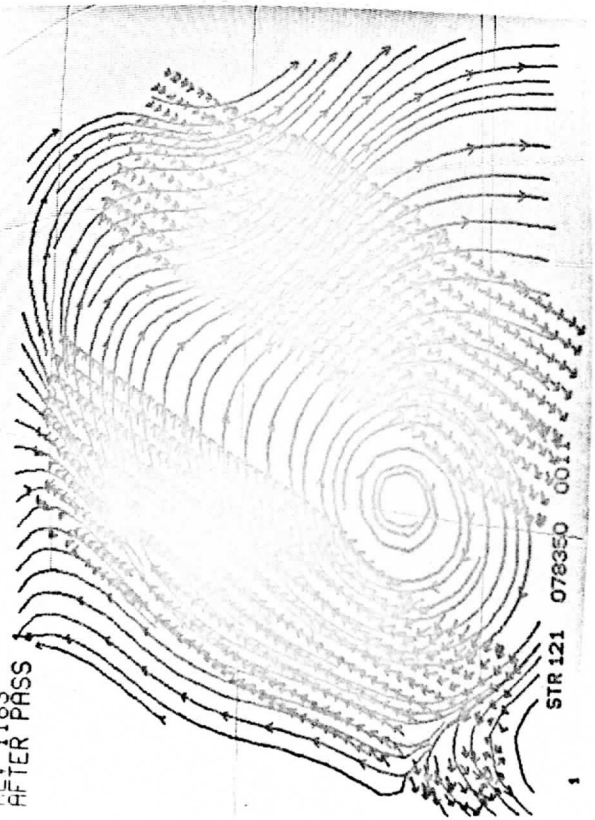
SIMULATED SCAT
REV 1183
TRUTH FIELD



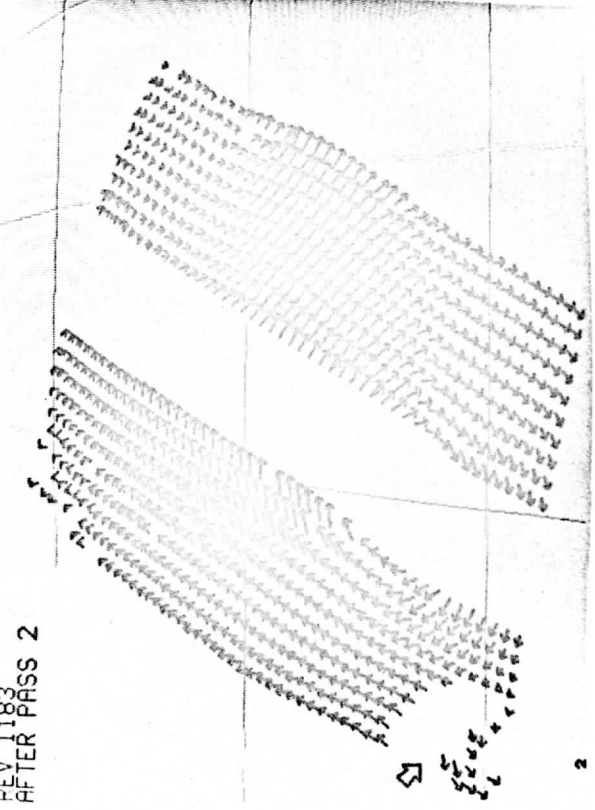
SIMULATED SCAT
REV 1183
FIRST GUESS FIELD



SIMULATED SCAT
REV 1183
AFTER PASS



SIMULATED SCAT
REV 1183
AFTER PASS 2



STR 121 078350 0011

Figure 7: Case 4, Rev 1183 upper half

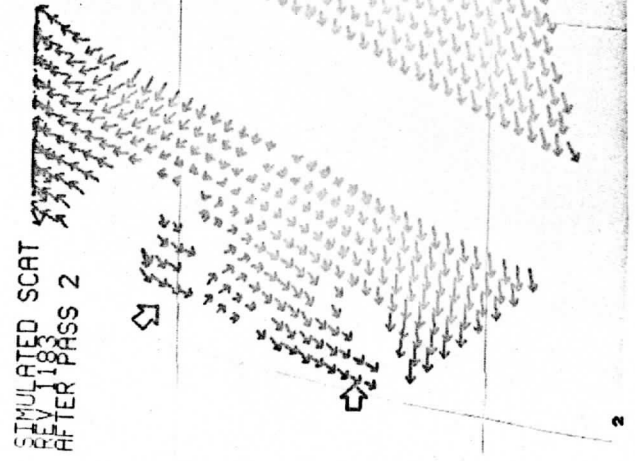
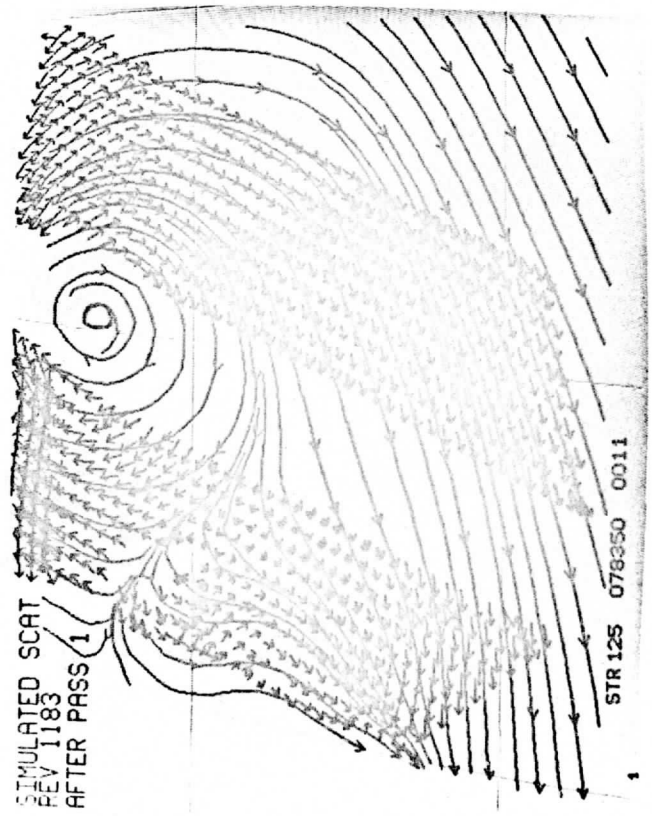
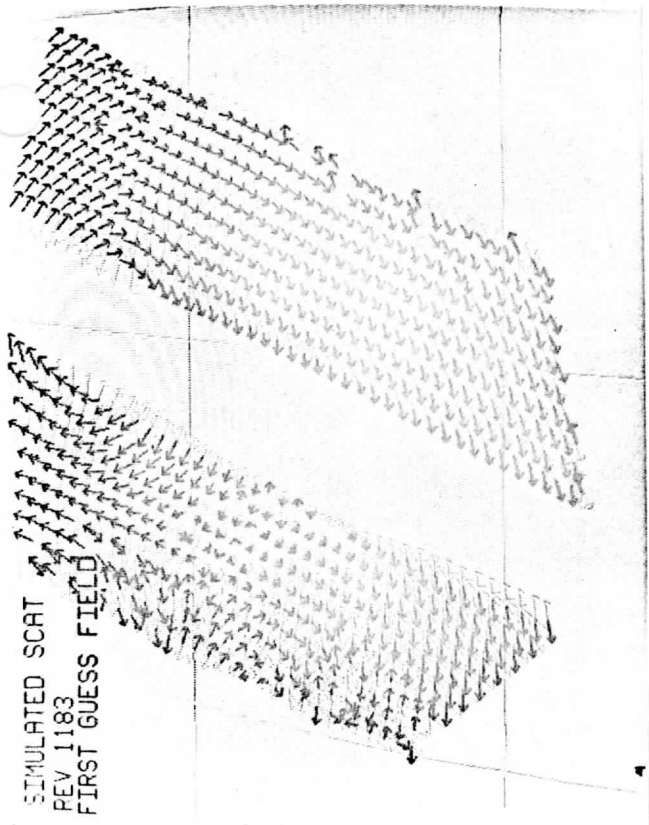
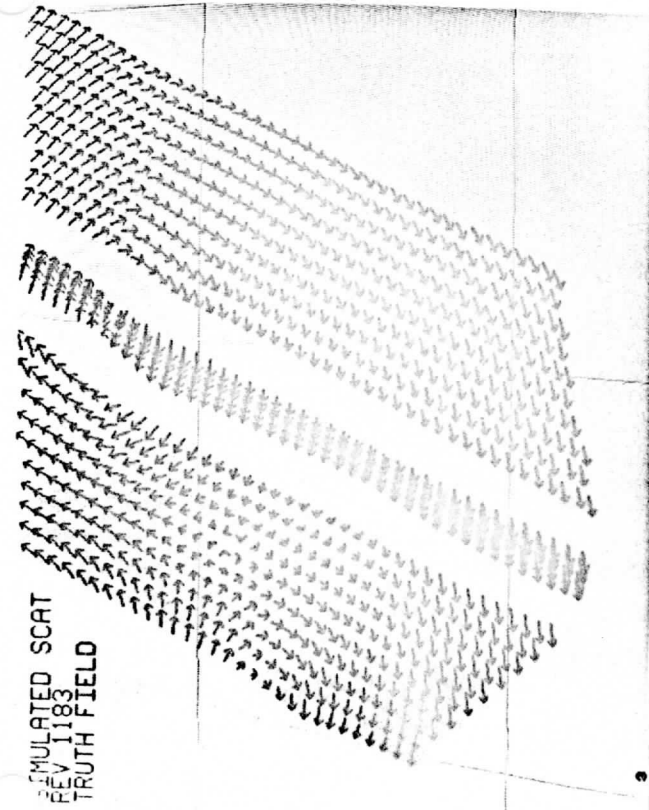
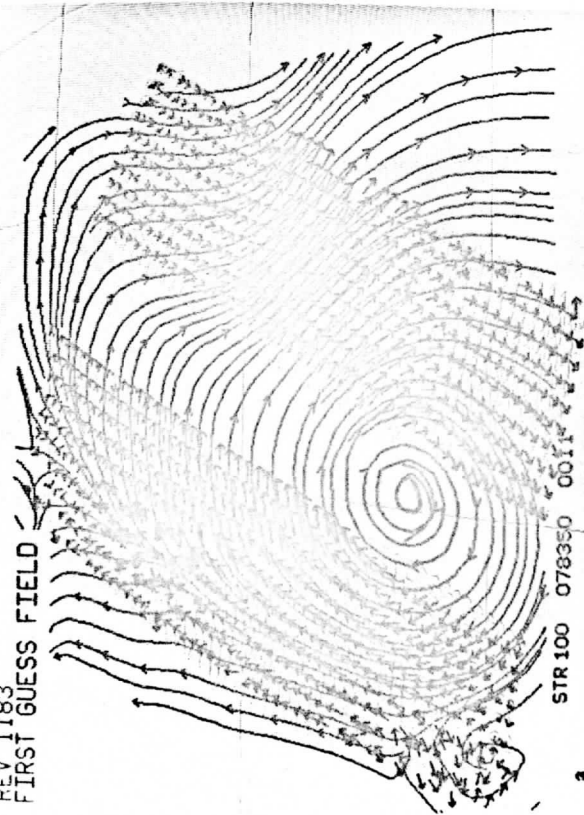


Figure 7 continued: Case 4, Rev 1183 lower half.

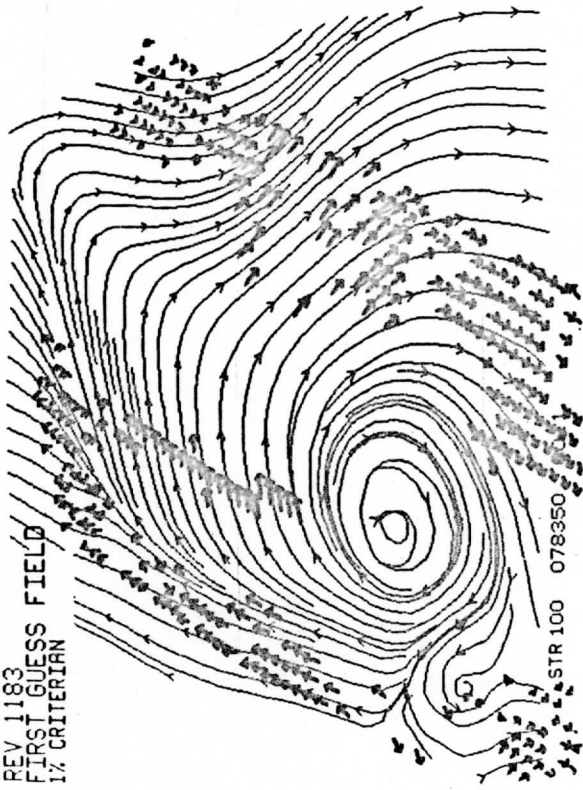
SIMULATED SCAT
REV 1183
FIRST GUESS FIELD



STR 100 078350 0011

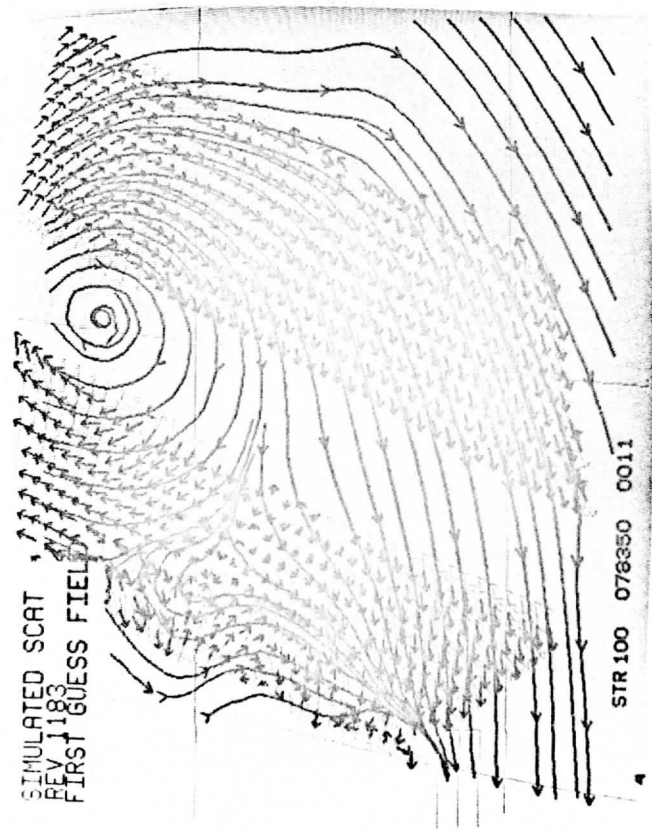
Upper

SIMULATED SCAT
REV 1183
FIRST GUESS FIELD
1% CRITERIAN



STR 100 078350

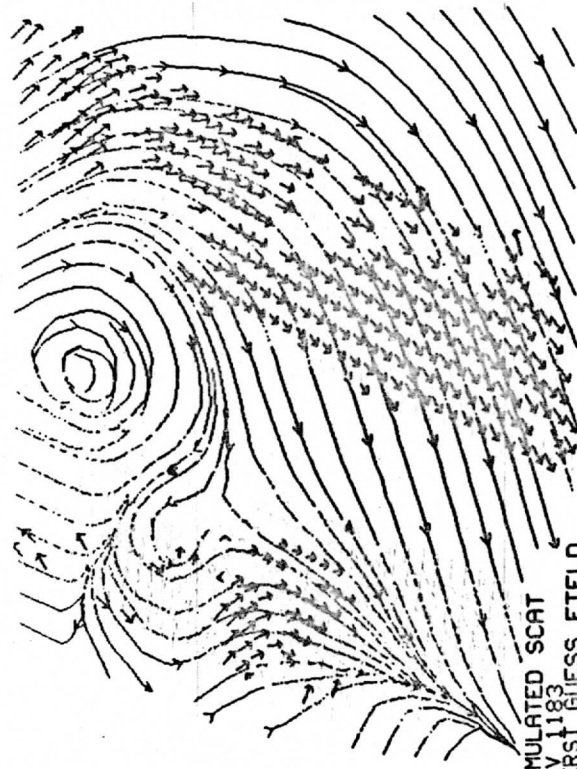
SIMULATED SCAT
REV 1183
FIRST GUESS FIELD



STR 100 078350 0011

Lower

SIMULATED SCAT
REV 1183
FIRST GUESS FIELD
1% CRITERIAN



350 0011

Figure 7: Continued -- Comparison of Normal 1st class to 1% criteria

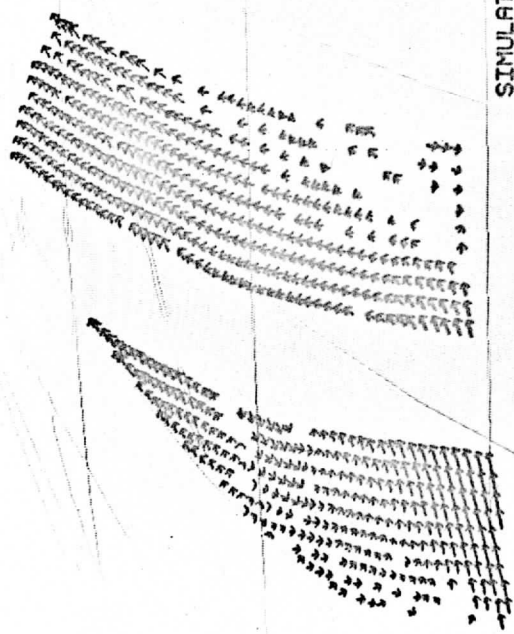
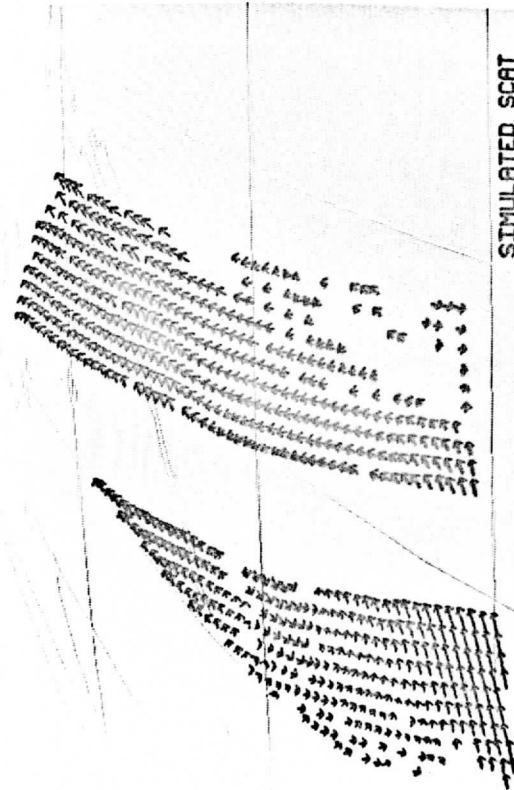
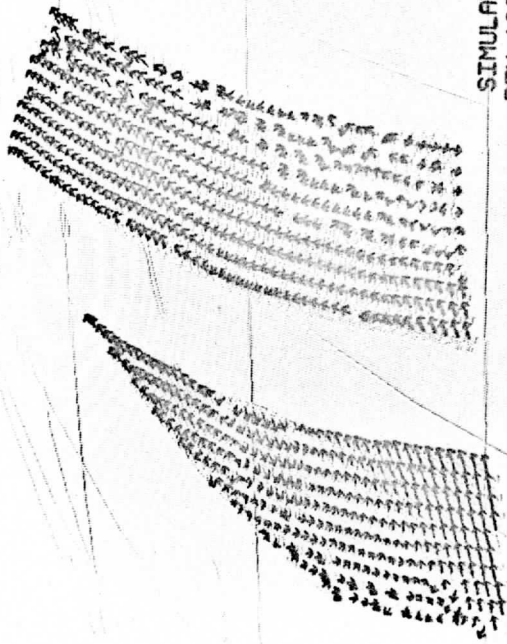
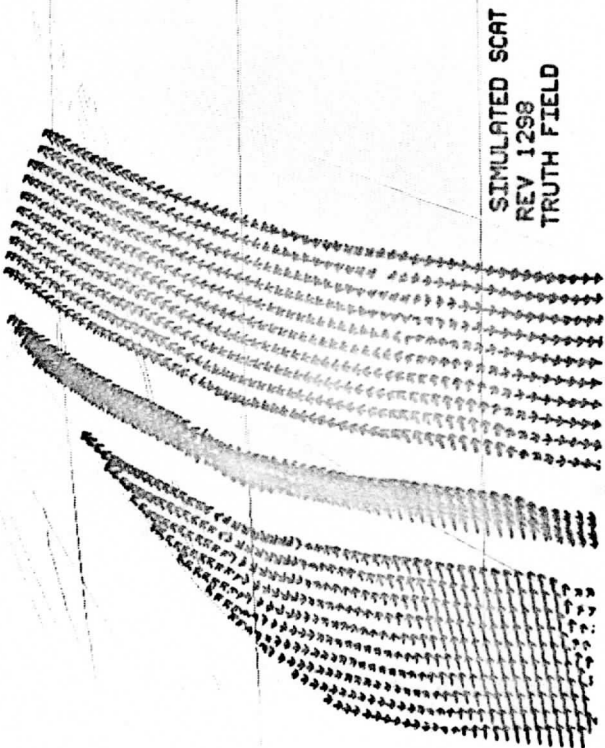


Figure 8: Case 5, Rev 1298 upper half

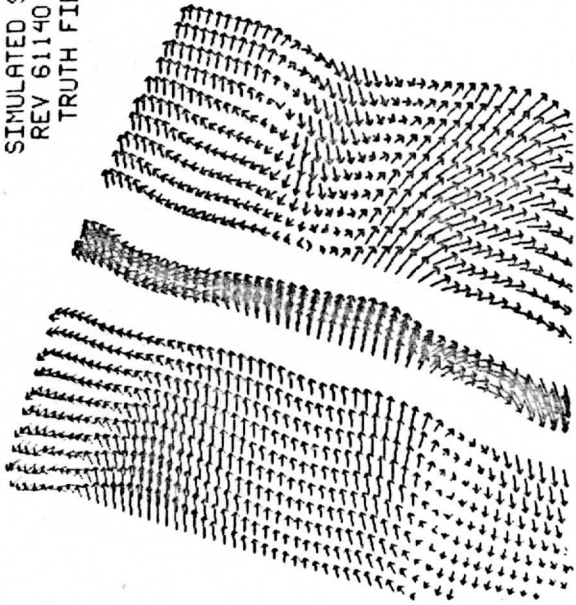
SIMULATED SCAT
REV 1298
FIRST GUESS FIELD

SIMULATED SCAT
REV 1298
TRUTH FIELD

SIMULATED SCAT
REV 1298
AFTER PASS 1

Figure 8 continued: Case 5, Rev 1298 lower half.

SIMULATED SCAT
REV 61140
TRUTH FIELD



SIMULATED SCAT
REV 61140
AFTER PASS 2

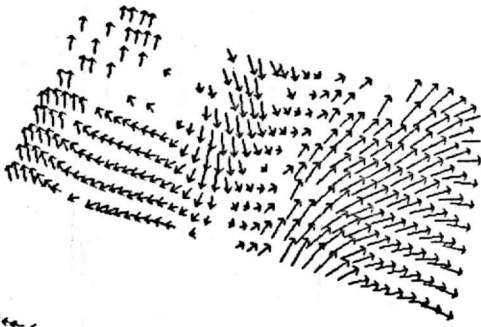
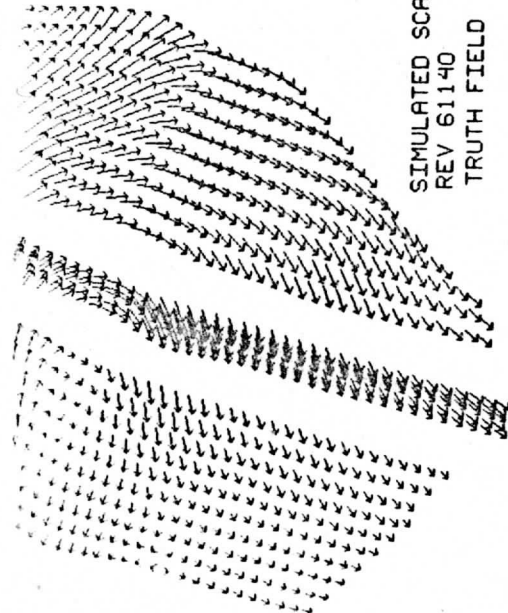


Figure 9: Case 6, Rev 1140 upper half.

SIMULATED SCAT
REV 61140
TRUTH FIELD



SIMULATED SCAT
REV 61140
AFTER PASS 2

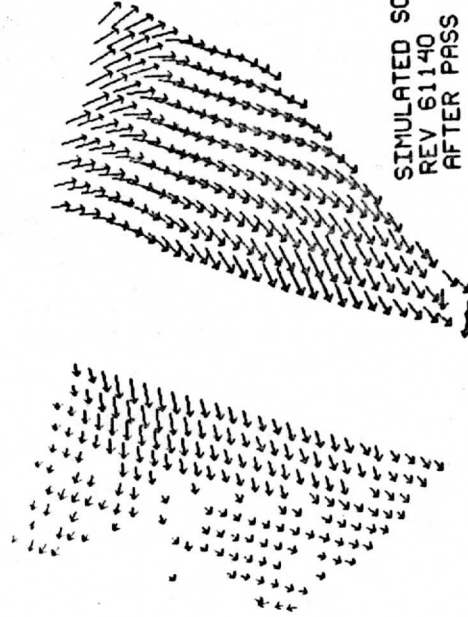


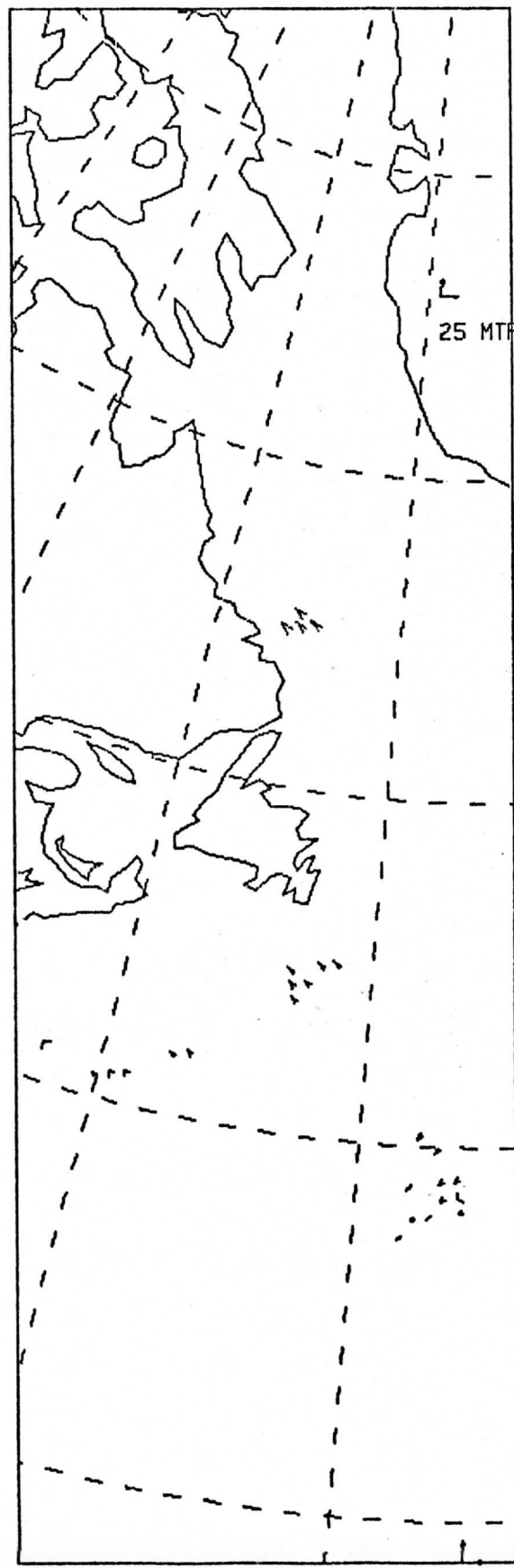
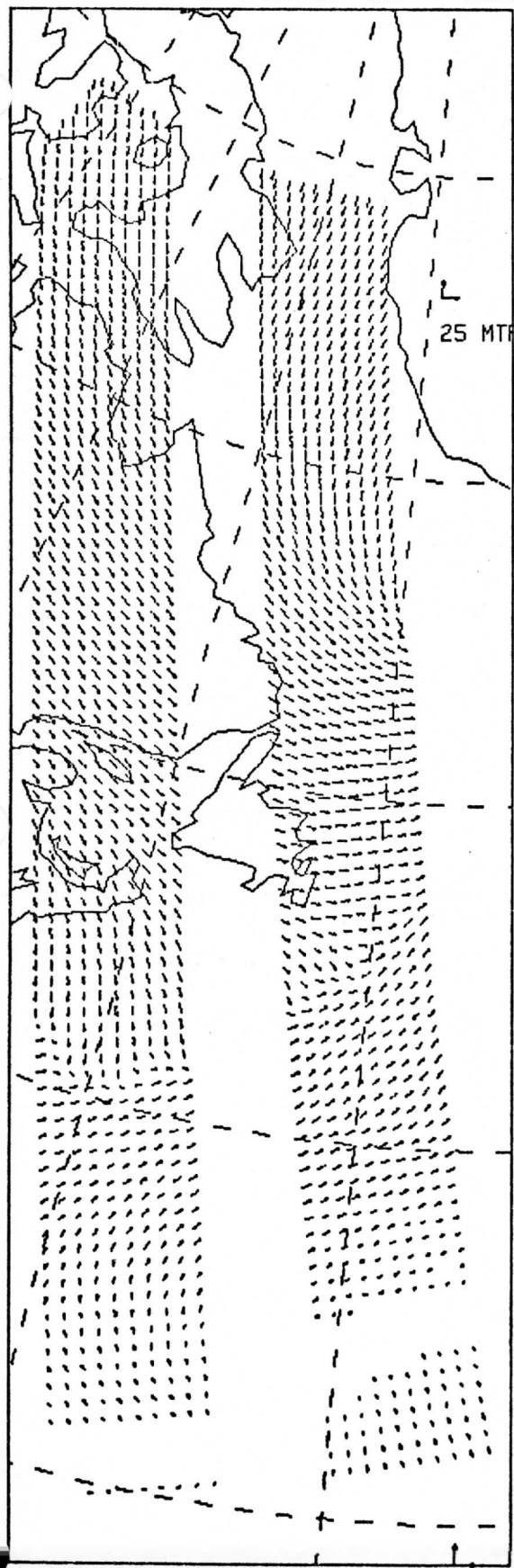
Figure 9 Case 6, Rev 1140 lower half.

Truth Field

Errors

WISC DATA - WITHHELD FLDS - CORRECT ALIAS -

WISC DATA -WITHHELD FLDS-PICK + PROPER ALIAS-



25 MTR/SEC

25 MTR/SEC

Figure 10. Blind data set case 1 truth vectors (left) and the locations of the bad picks (right). Both chosen alias and the proper alias are plotted on the right.

9/1/82

Case 2 Blind Set

Truth Vectors

MISC DATA - WITHHELD FLDY - CORRECT ALIAS -

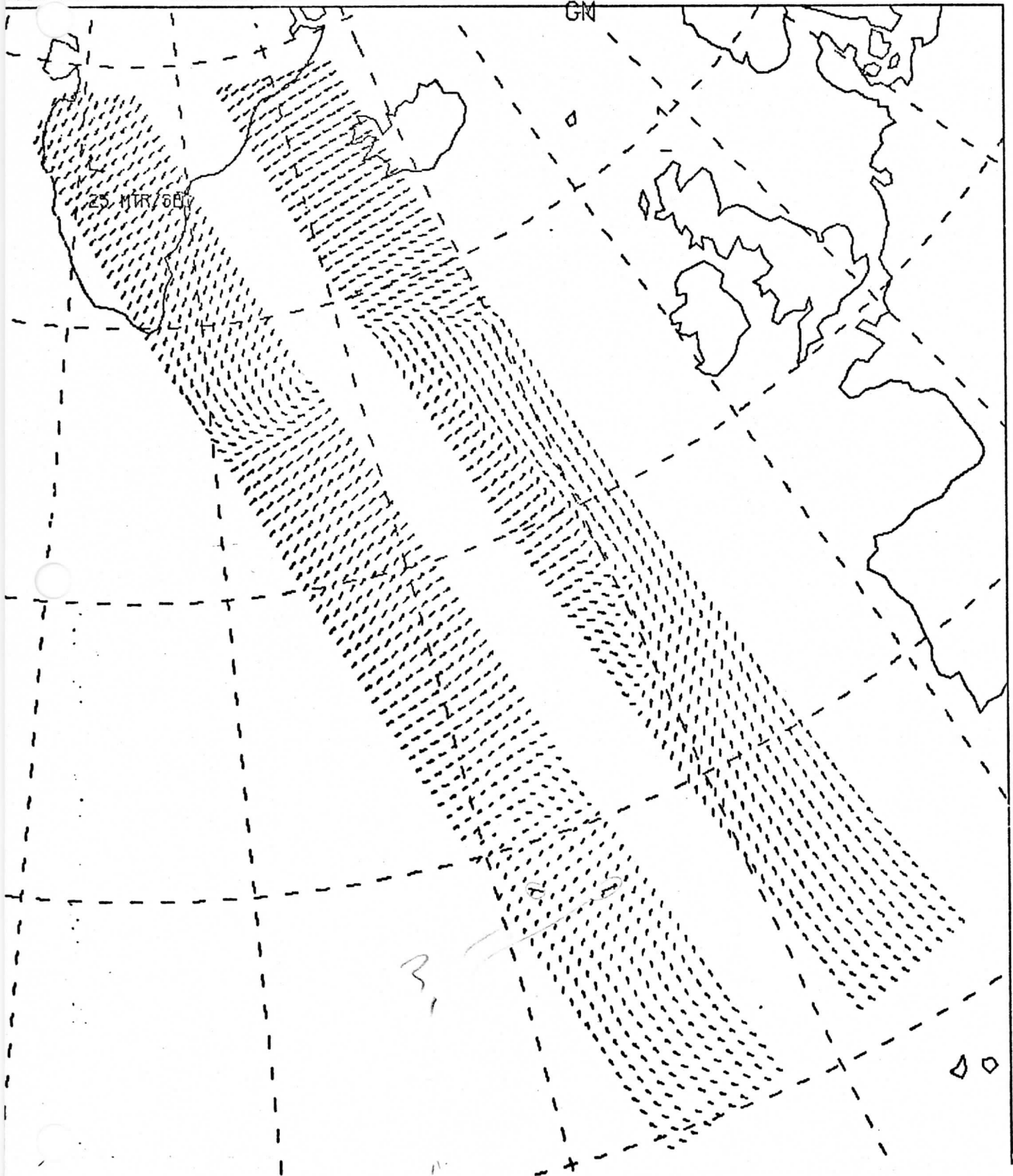


Figure 11a. Blind data set case 2 truth field.

25 MTR/SEC

Case 2 Blind Set
Bad Picks

WISC DATA -WITHHELD FLD2-PICK + PROPER ALIAS-

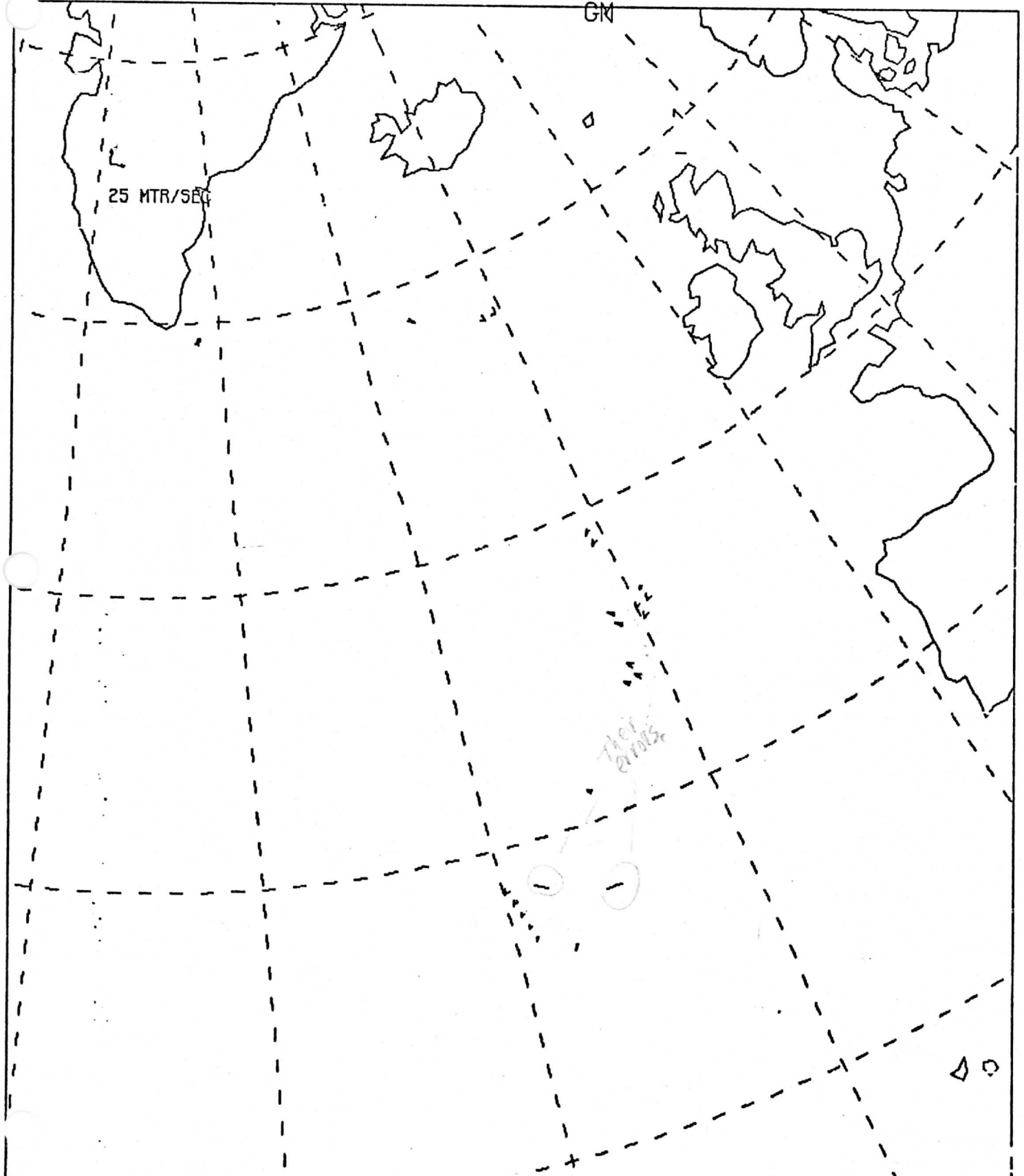


Figure 11b. Blind data set case 2 bad pick locations.

25 MTR/SEC

Case 3

9/1/02

Truth Vectors

WISC DATA - WITHHELD FLD3 - CORRECT ALIAS -

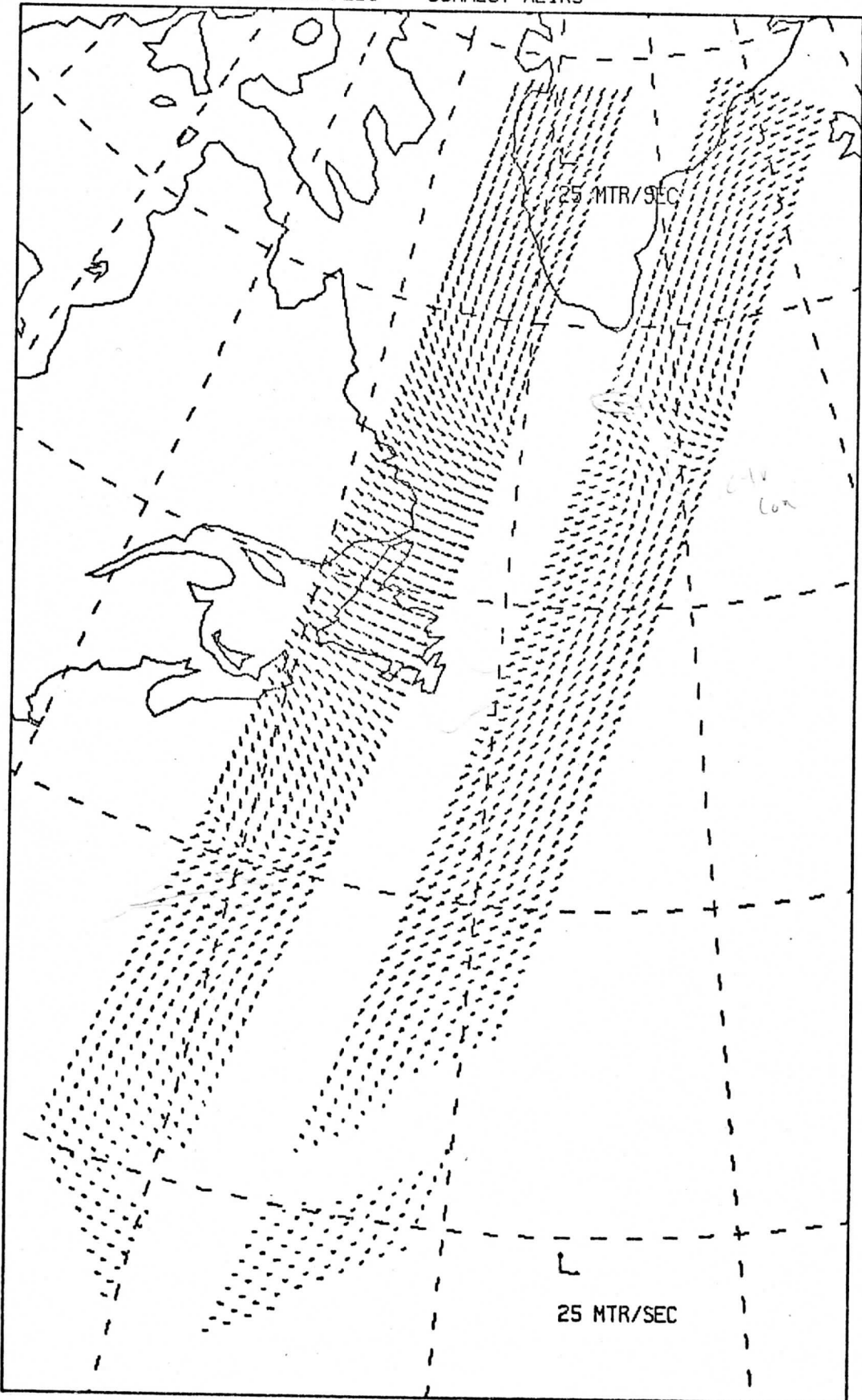


Figure 12a. Blind data set case 3 truth vectors.

Case 3 Blind set

Bad Picks

WISC DATA -WITHHELD FLD3-PICK + PROPER ALIAS-

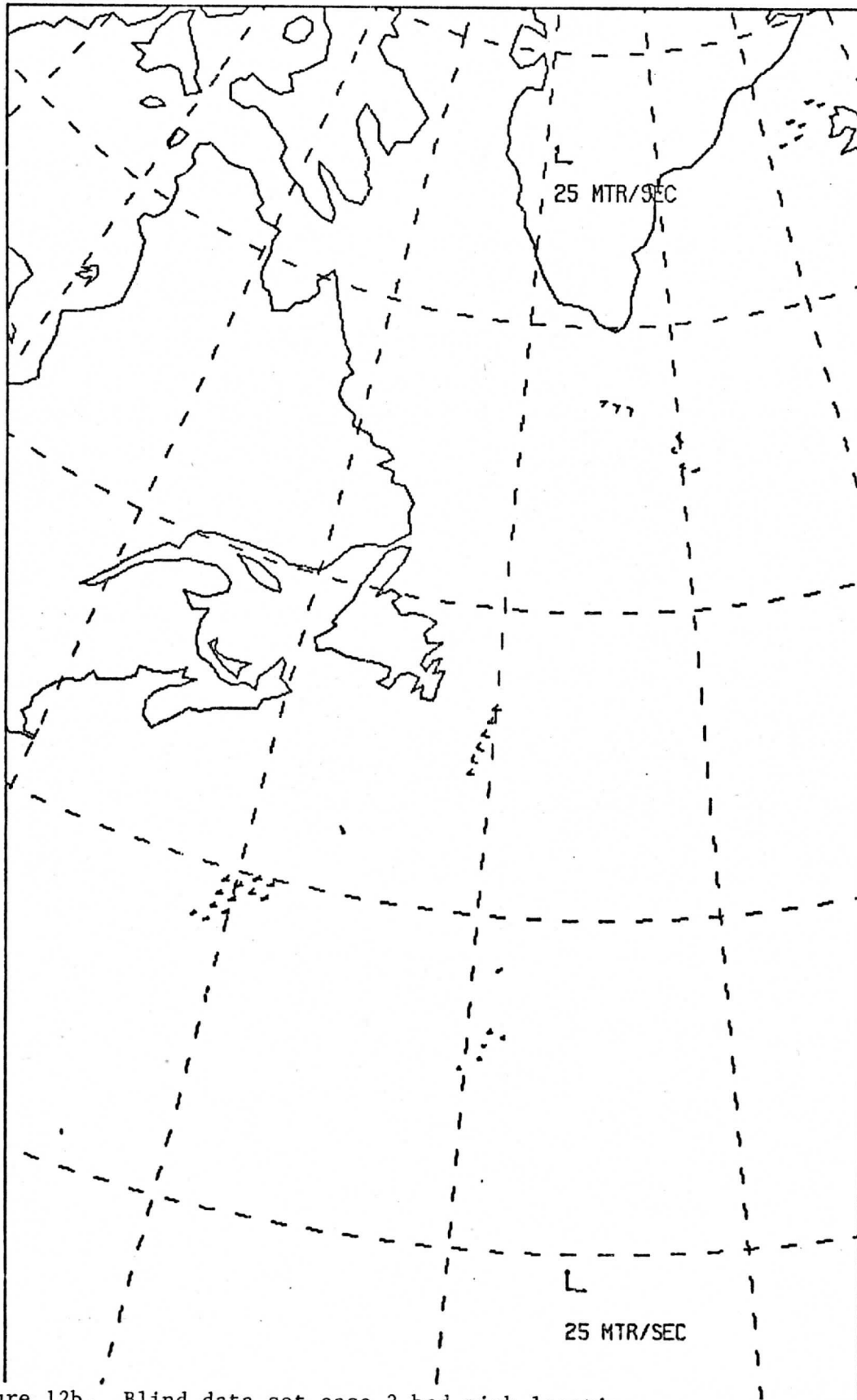


Figure 12b. Blind data set case 3 bad pick locations.

Case 4 Blind Set

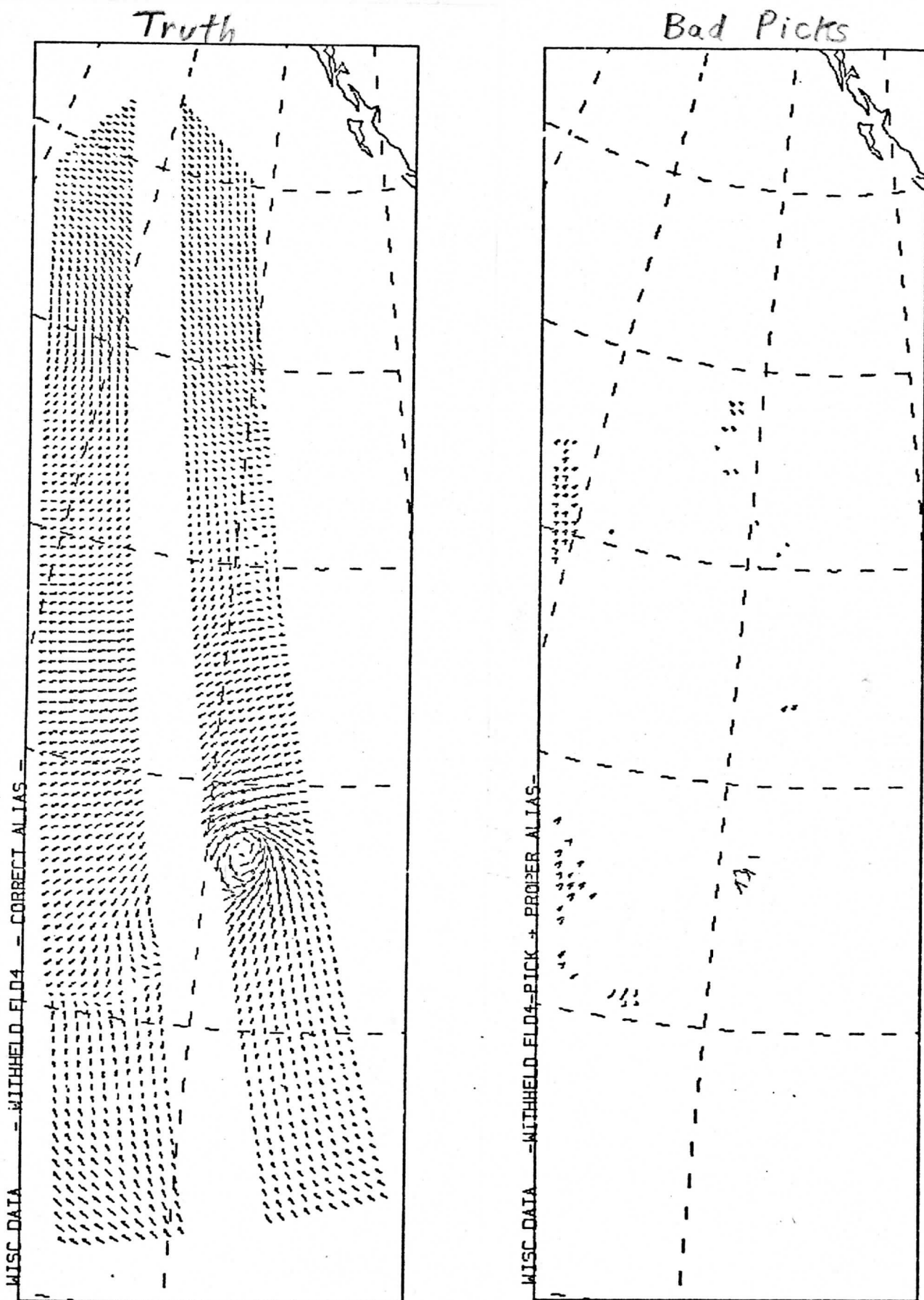


Figure 13. Blind data set case 4 truth vectors (top) and bad pick locations (bottom).

Case 5

Truth

Bad Picks

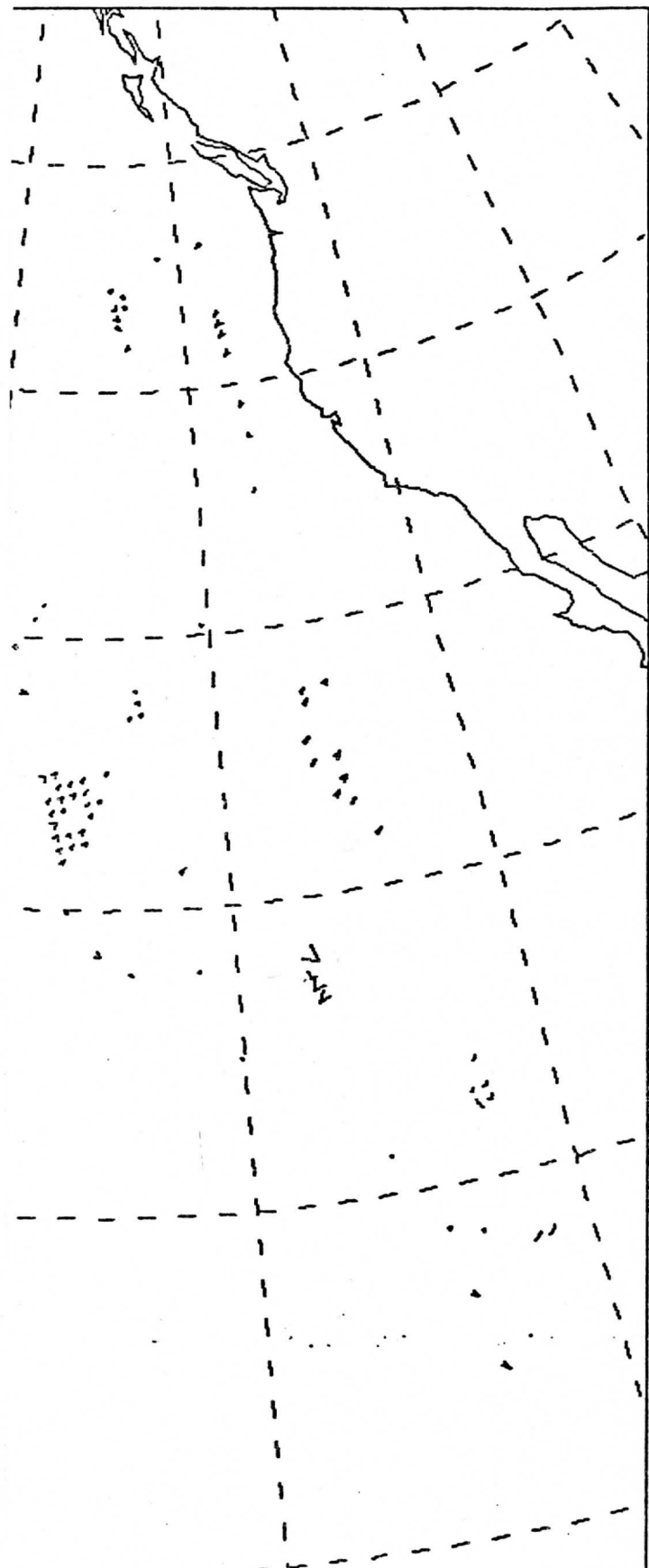
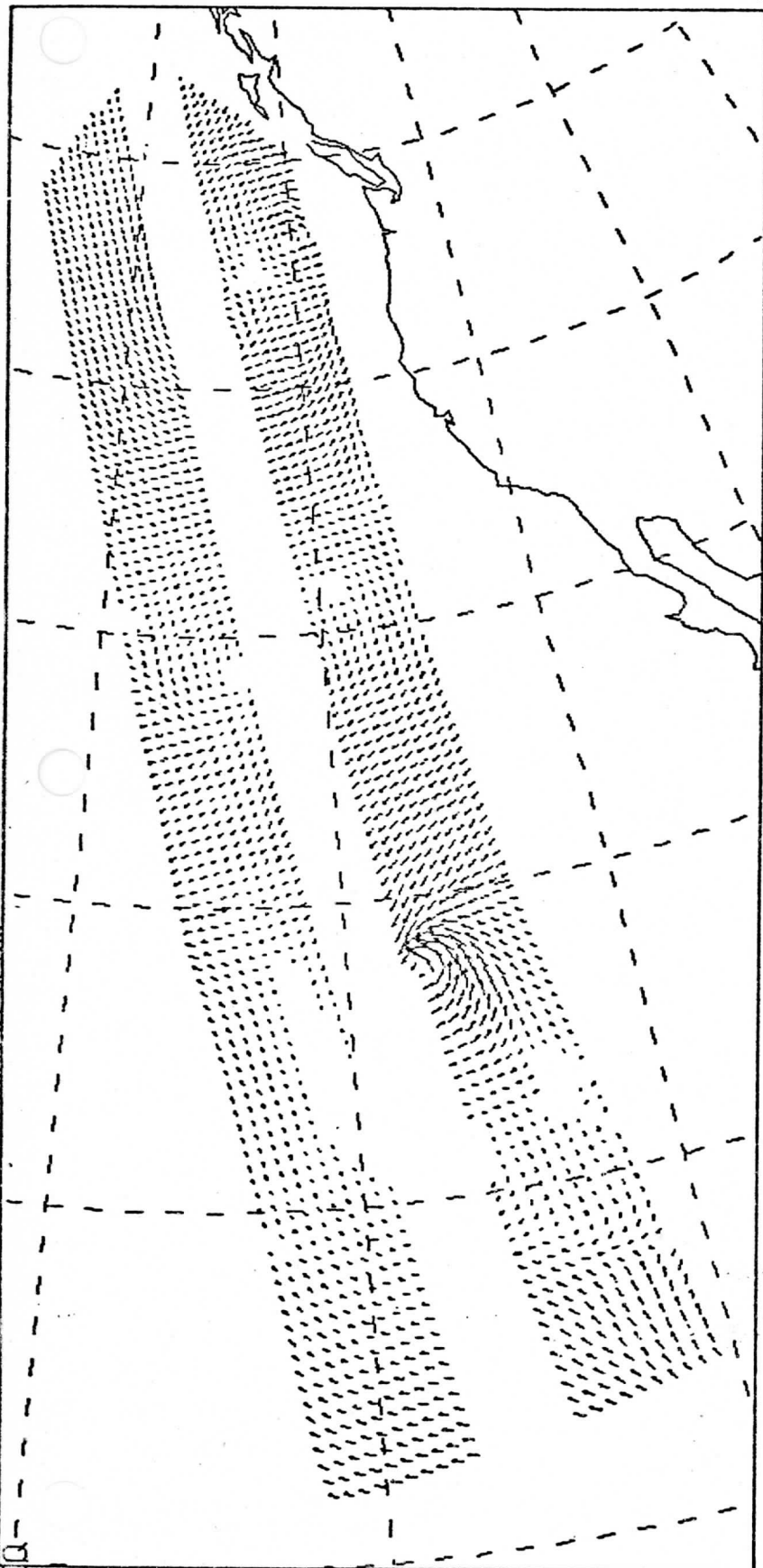
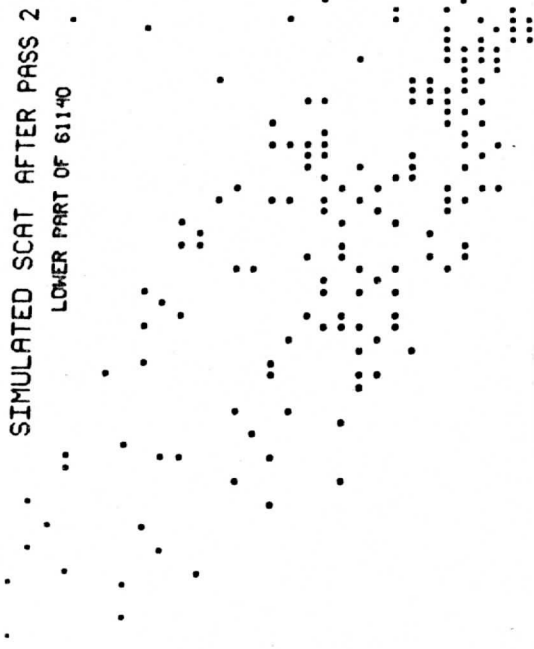
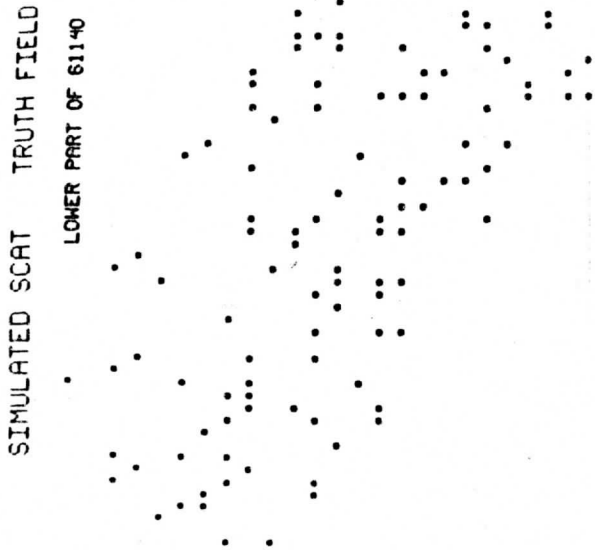
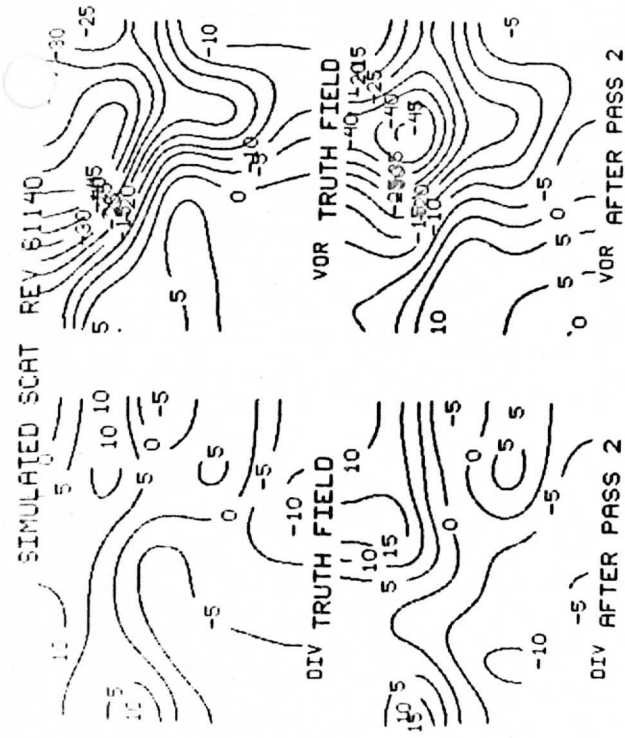
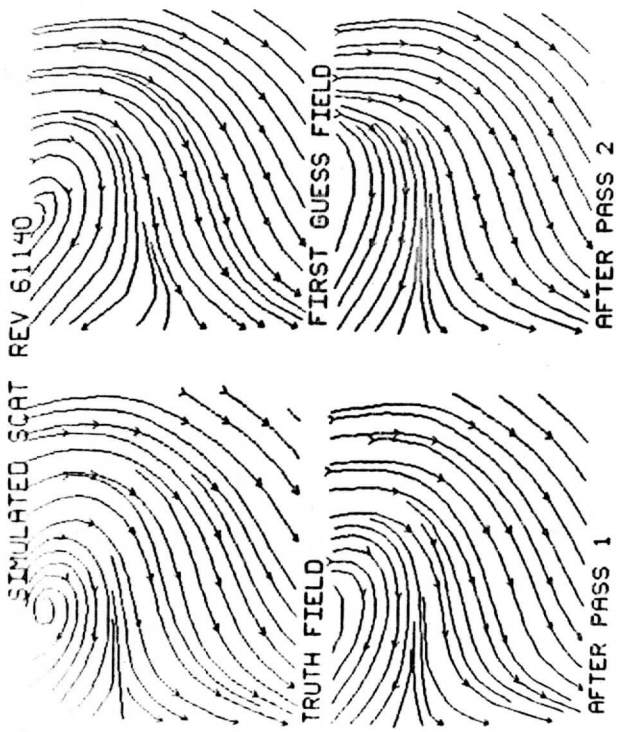


Figure 14. Blind data set case 5 truth vectors (top) and bad pick locations (bottom).



VORTICITY

VORTICITY

Figure 15. Example vorticity and divergence analyses. The left panels are divergences and the right panels are vorticities. The top row was made from the truth field, while the bottom row was made from the edited vectors. The scatter plots of divergence (ordinate) vs. vorticity (abscissa) are from the truth field on the left and the edited data on the right.

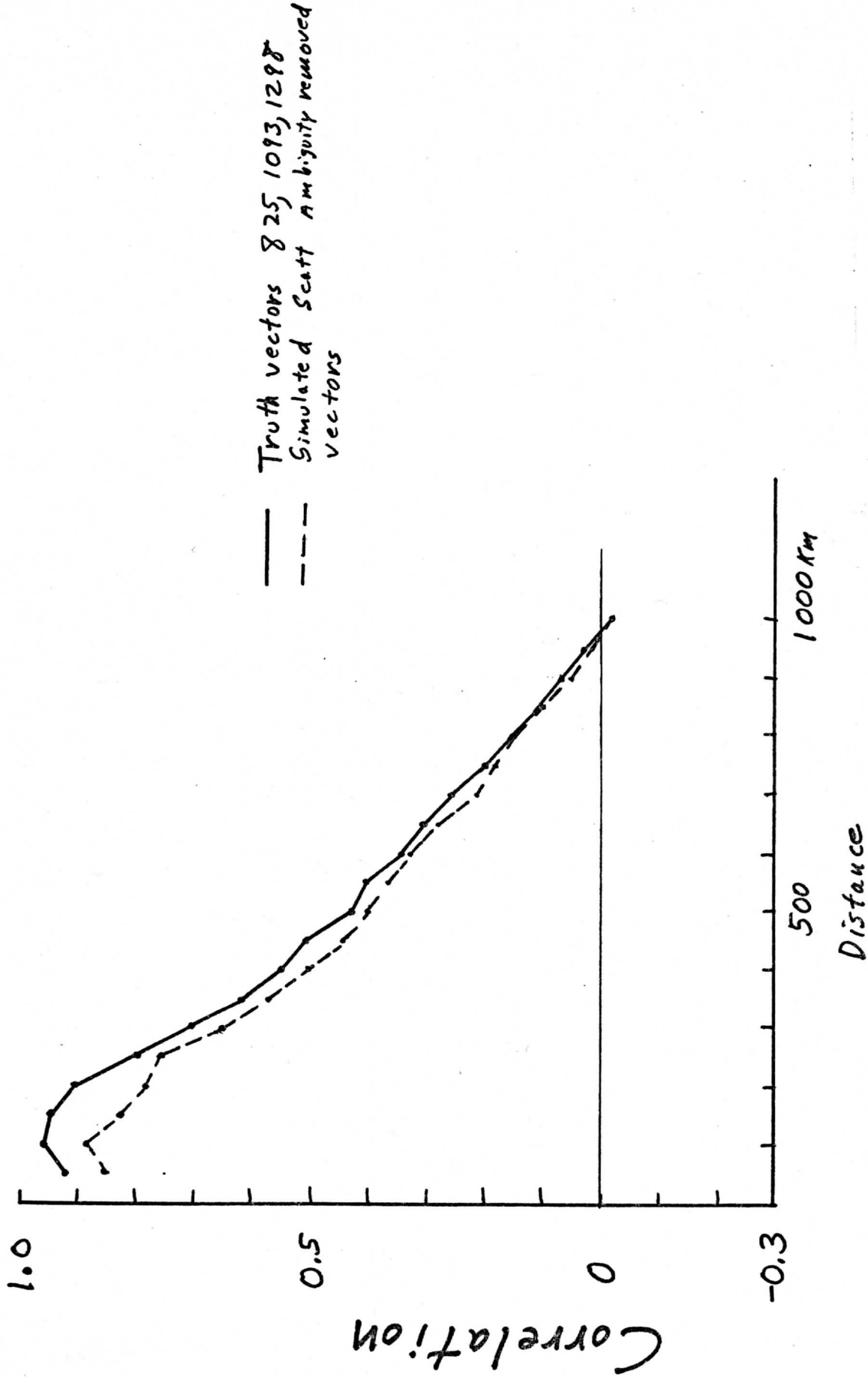
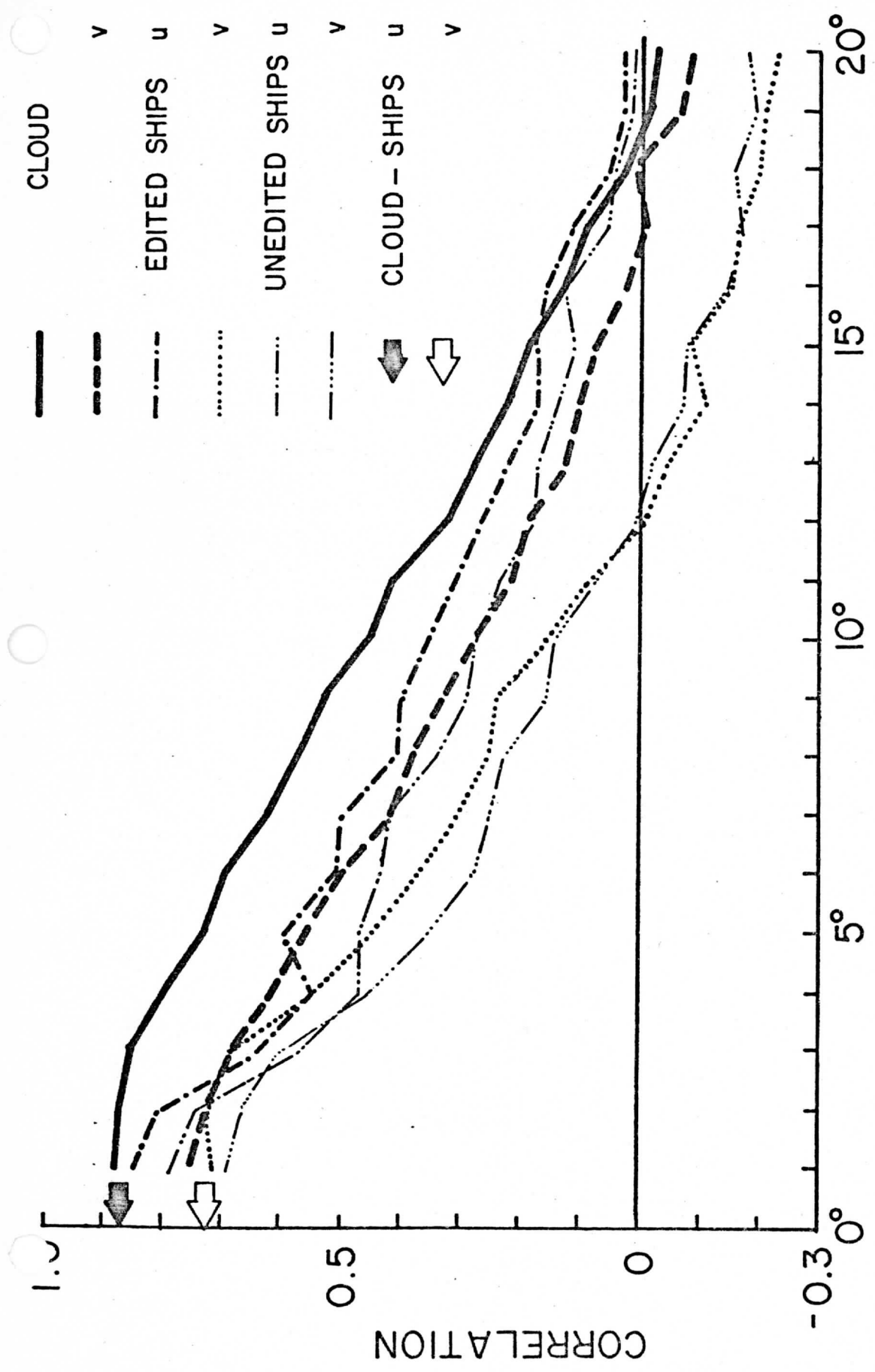


Figure 16. The auto correlations of the Truth and edited SCATT vectors.



SEPARATION DISTANCE (LAT., LONG.)

Figure 17. The auto correlations of cloud motion vectors and ship reports in the Indian Ocean for the months of May, June, and July 1979. Taken from Wylie and Hinton (1981).